

CALCULATIONS OF NEUTRON EMISSION IN FISSION

CALCULATIONS OF NEUTRON EMISSION
IN THE
THERMAL NEUTRON FISSION OF U^{235}

By

CALVIN DAVID BRUBAKER, B.Sc.

A Thesis

Submitted to the Faculty of Graduate Studies
in Partial Fulfilment of the Requirements
for the Degree
Master of Science

McMaster University

October 1960

Master of Science (1960)
(Physics)

McMaster University
Hamilton, Ontario

Title: Calculations of Neutron Emission in the Thermal Neutron
Fission of U^{235}

Author: Calvin David Brubaker, B.Sc. (McMaster University)

Supervisor: Professor M. A. Preston

Number of Pages: viii, 55

Scope and Contents:

The probability of fission as a function of primary fragment velocities has been obtained by removing the neutron emission and instrumental dispersions from the velocities determined by Stein with time-of-flight techniques for the thermal neutron fission of U^{235} . Each velocity was increased by 0.69% to make the average kinetic energy per fission agree with the calorimetric value of 167.1 Mev. Excitation energy distributions were obtained by using the primary fragment masses given by Cameron and assuming that the most probable charge distribution for a given mass ratio is that which leads to the greatest energy release. Evaporation theory was used to determine the number of prompt neutrons emitted. When the excitation energy is divided equally between the fragments and a nuclear temperature of 0.59 Mev is used, the average number of neutrons emitted is 2.95 per fission.

Acknowledgments

I sincerely wish to thank Professor M. A. Preston for the constructive criticism and guidance received from him throughout this work.

Thanks are due to William E. Stein who supplied me with the experimental data used in the present analysis.

I am grateful to Imperial Oil Limited for their generous financial support.

The calculations involved in this work were performed using the Bendix G-15D digital computer located at McMaster University. The author appreciates the assistance of Edward M. Beaver who maintained the computer in good electronic condition.

Table of Contents

I	Introduction	1
II	Analytic Form for the Velocity Probability Surface	3
III	Dispersions to be Removed from the Velocity Probability Surface	6
	1. Dispersion due to Instrumental Errors	6
	2. Dispersion due to Neutron Emission	7
	3. Total Dispersion to be Removed	9
	4. Velocity Loss due to Nickel Source Backing	11
IV	Removal of Dispersions from Velocity Probability Surface	11
V	Kinetic Energy Distributions	13
	1. Kinetic Energy Distribution at Constant Mass Ratio	13
	2. Adjustment of Velocities to Yield Calorimetric Average Kinetic Energy	14
	3. Example of Dispersion Removal in Kinetic Energy Distributions	17
	4. Simplified Analytic Form for Certain Kinetic Energy Distributions	17
VI	Total Energy Release in Fission	18
	1. Total Energy Release in a Particular Fission Mode	18
	2. Charge Distribution for a Given Mass Ratio	19
	3. Mean Total Energy Release for a Given Mass Ratio	20
VII	Single Fragment Excitation Energy Distributions	21
VIII	Conditional Neutron Emission Probabilities	22
IX	Neutron Emission Calculations	25
	1. Method of Calculation	25

2. Parameters Involved in Calculations	26
3. Mean Values for Separation Energies and Total Energy Release	27
4. Dependence of Neutron Emission on Nuclear Temper- ature	28
5. Dependence of Neutron Emission on Division of Total Excitation Energy between Fragments	30
6. Dependence of Neutron Emission on Mean Total Energy Release	31
7. Neutron Emission Calculations for Fourteen Mass Ratios	32
X Discussion of Neutron Emission Calculations	32
1. Comparison of Calculations with Experimental Determinations	32
2. Cumulative Yield Curves	35
3. Conclusions	36
Tables	39
Figures	46
Bibliography	55

List of Tables

I	Coefficients for the Velocity Probability Surface $F_0(x,y)$	39
II	Importance of Velocity Dispersion in Heavy Fragment Velocities	40
III	Importance of Velocity Dispersion in Light Fragment Velocities	41
IV	Constants in the Total Kinetic Energy Probability Density Functions $Q_K(E_K^t; R)$	42
V	Validity of Using Mean Energies in Neutron Emission Calculations for Mass Ratio $R = 143/93$	43
VI	Dependence of Neutron Emission on Nuclear Temperature for Fission with Mass Ratio $R = 143/93$	44
VII	Dependence of Neutron Emission on Excitation Energy Division for Fission with Mass Ratio $R = 143/93$	44
VIII	Dependence of Neutron Emission on Mean Total Energy Release for Fission with Mass Ratio $R = 143/93$	45

List of Figures

1. Dispersion Removal in Kinetic Energy Probability Density Function for Mass Ratio $R = 143/93$ 46
 - a. Function after Dispersion Removal
 - b. Function before Dispersion Removal
2. True Kinetic Energy Probability Density Functions $Q_K(E_K^t; R)$ for Mass Ratios with Heavy Fragment Mass Numbers 127, 129, 131, 133, 135, and 137 47
3. True Kinetic Energy Probability Density Functions $Q_K(E_K^t; R)$ for Mass Ratios with Heavy Fragment Mass Numbers 139, 141, and 143 48
4. True Kinetic Energy Probability Density Functions $Q_K(E_K^t; R)$ for Mass Ratios with Heavy Fragment Mass Numbers 145, 147, 149, 151, and 153 49
5. Mean Total, Kinetic and Excitation Energies at Fourteen Mass Ratios, as a Function of the Heavy Fragment Mass Number 50
6. Energy Diagram for the Conditional Neutron Emission Probability $p(3; \beta_3 \leq E \leq \beta_4)$ 51
7. Excitation Energy Distribution and Conditional Neutron Emission Probabilities for the Fragment with Mass Number 93, using $r = 0.5$ 52
 - a. Nuclear Temperature $T = 0.59$
 - b. Nuclear Temperature $T = 1.00$
8. Excitation Energy Distribution and Conditional Neutron Emission Probabilities for the Fragment with Mass Number 143, using $r = 0.5$ 53

a. Nuclear Temperature $T = 0.59$

b. Nuclear Temperature $T = 1.00$

9. Neutron Emission from Individual Fragments at Fourteen Mass

Ratios, using $r = 0.5$, $T = 0.59$, and $\Delta\bar{E}_T = 0$

54

I Introduction

The principle of conservation of energy applied to the fission of the compound nucleus $M(A,Z)$ can be expressed by the equations

$$M(A-1,Z) + N + E_n = M_H(A_H,Z_H) + M_L(A_L,Z_L) + E_K^t + E_X^t,$$

$$A_H + A_L = A, \text{ and } Z_H + Z_L = Z,$$

where N and E_n are the mass and kinetic energy of the thermal neutron which induces fission, M_H and M_L are the ground state masses of the primary fission fragments and E_K^t and E_X^t are the kinetic and excitation energies of the primary fragments. The kinetic energy of the thermal neutron is negligible compared with the other energies, and is therefore dropped from the above equation. The neutron mass is 1.00898 amu, and the mass $M(A-1,Z)$ is known with fair accuracy. Since the primary fragments are neutron-rich and emit prompt neutrons within less than about 10^{-15} seconds after their formation, the masses of these fragments are not known experimentally and must be determined by extrapolations from measured masses. As for the kinetic energies, any attempts to measure them result in the inclusion of errors which must then be removed if the energies are to be used in the conservation of energy equation. However, if the true energies E_K^t are inserted in the above equation one can obtain the corresponding excitation energies E_X^t . In some cases probability distributions for the energies E_K^t have been determined experimentally, and the probability distributions for the energies E_X^t can then be derived. Although one can apply the principle of conservation of momentum to the primary fission fragments and thereby obtain the kinetic energy distribution for each fragment, there is no such known relationship which could be used to determine the single

fragment excitation energy distributions. However, if one assumes a certain division of excitation energy between the fragments one can then proceed by evaporation theory to calculate the number of neutrons which are expected to be emitted by each fragment. A comparison of the calculated neutron multiplicities with those measured experimentally constitutes a check on the analysis.

The first reliable kinetic energy data for the thermal neutron fission of U^{235} were obtained by Brunton and Hanna (1950) using a double ionization chamber and assuming that fission fragment energies are proportional to the ionization produced. However, it has been shown by Schmitt and Leachman (1956) that for fission fragments slowed in an ionization chamber an ionization defect occurs which is most important toward the end of the range of the fragments. Here the energy loss by non-ionizing processes becomes quite important and the relationship between the fragment kinetic energy and the ionization produced should not be assumed to be linear.

Leachman (1956) and Leachman and Kazek (1957) have performed calculations to determine the excitation energy distributions and the number of neutrons emitted by the primary fission fragments from several fissile materials, including U^{235} . They base their fission fragment kinetic energy distributions on ionization chamber data and assume that the excitation energy distributions of both fragments are the same. They then calculate the probabilities that certain fragments near the most probable mass division emit 0, 1, 2, ... neutrons, and average these probabilities over the mass divisions considered. The ionization defect in the data they used was adjusted to make their calculated

average number of neutrons per fission agree with the value determined experimentally. However, it would be more satisfactory if one did not have to use an arbitrary ionization defect in order to obtain such agreement.

The ionization chamber method of obtaining fission fragment kinetic energies has now been replaced by the time-of-flight technique by which one obtains the time required for a fragment to travel a known distance. The velocities obtained by this method are those of the fragments after the emission of prompt neutrons and hence must be corrected before being used in the conservation of energy equation. However, the energies derived from time-of-flight velocities have a better resolution than those from ionization chamber experiments and also there is no large energy shift such as ionization defect.

Stein (1957) has used the time-of-flight technique to obtain the velocities of pairs of fission fragments for the thermal neutron fission of U^{233} , U^{235} , and Pu^{239} . With his apparatus a fission fragment whose velocity is to be measured passes down one of two collinear drift tubes. The time of occurrence of each fission is recorded by detecting the electrons which are ejected from the fissile source as the fragments emerge from it. A second time determination is made on pairs of fragments which travel 269 cm down the drift tubes to the fragment detectors of 2 inch and 8 inch diameter. The calculations discussed in this thesis are based on the 3050 velocity pairs obtained by Stein for the thermal neutron fission of U^{235} .

II Analytic Form for the Velocity Probability Surface

The description is now given of how the velocity pairs (v_H^0 , v_L^0)

of the heavy and light fission fragments taken from Stein's experiment for the thermal neutron fission of U^{235} were plotted on a grid in the $v_H^0 v_L^0$ plane, and how an analytic function for the velocity probability surface was obtained.

A grid was formed by parallel lines 0.5×10^7 cm/sec apart, one set of lines drawn parallel to the v_H^0 axis and the other set parallel to the v_L^0 axis. The basic squares so formed were grouped to form larger squares with sides of length 3.0×10^7 cm/sec parallel to the co-ordinate axes. The size of these large squares was determined by the number of velocity pairs available. It was a compromise between smaller squares which would give rise to unnatural fluctuations in probabilities among adjacent squares, and larger squares which would smooth out any true fluctuations in the probabilities. The height of the probability surface at the mid-point of each large square was then taken as proportional to the number of velocity pairs which occurred in that square.

By taking cross sections of the probability surface it was found that the surface had approximate symmetry with respect to a system of axes obtained by rotating the $v_H^0 v_L^0$ axes clockwise through the angle $\alpha = \arctan 3/5 \approx 31^\circ$ and by translating the origin to the point with co-ordinates $v_H^0 = 0.9605 \times 10^7$ cm/sec, $v_L^0 = 1.4095 \times 10^7$ cm/sec. The transformation from the experimental velocities v_H^0 and v_L^0 to the velocities $v_H^{0'}$ and $v_L^{0'}$ with respect to these symmetry axes is therefore given by

$$\begin{aligned} v_H^{0'} &= (v_H^0 - 0.9605 \times 10^7) \cos \alpha - (v_L^0 - 1.4095 \times 10^7) \sin \alpha \\ v_L^{0'} &= (v_H^0 - 0.9605 \times 10^7) \sin \alpha + (v_L^0 - 1.4095 \times 10^7) \cos \alpha. \end{aligned}$$

In carrying out the analysis a change of scale along the symmetry axis was introduced. The basic unit in this new system is equal to the

distance between the centres of adjacent grid squares. One defines

$$2 \text{ pseudounits} = 3 \times 10^7 \text{ cm/sec,}$$

so that the pseudounit co-ordinates x and y are given by

$$x = \frac{2}{3 \times 10^7} v_H^0,$$

$$\text{and } y = \frac{2}{3 \times 10^7} v_L^0.$$

Cross sections of the probability surface were taken along various lines parallel to both symmetry axes and it was found that, except for two high regions located symmetrically about the y axis on the x axis, the surface could be represented by a function of the form

$$f_0(x,y) = (A_0 + A_{10}x + A_{01}y + A_{20}x^2 + A_{11}xy + A_{02}y^2 + A_{21}x^2y + A_{12}xy^2 + A_{22}x^2y^2) e^{-\left(\frac{x^2}{60} + \frac{y^2}{20}\right)},$$

where the numbers occurring in the exponential were chosen to make the coefficients A_{ij} small. Furthermore, it was found that one could take A_{11} and A_{22} to be zero, and this was done. The coefficients in the above function were then obtained by a least squares fit of the function to the probabilities given at the mid-point of each square in two grid systems. Each grid was formed with squares of sides 3×10^7 cm/sec in length as previously described. The first grid contributed 183 points to the least squares fit and the second grid, formed by squares whose centres fall on the corners of the squares of the first grid, contributed an additional 190 points. The two sets of grids were used in order to obtain more reliable coefficients than one set would have given. The results of the least squares fit were that the coefficient A_{10} was negligible and that a new term should be added to the function $f_0(x,y)$ in order to take account of the two high regions to which reference has already been made.

The least squares procedure described above was applied to the function

$$F_0(x,y) = (A_0 + A_{01}y + A_{20}x^2 + A_{02}y^2 + A_{21}x^2y + A_{12}xy^2) e^{-\left(\frac{x^2}{60} + \frac{y^2}{20}\right)} + Bx^2 e^{-\left(\frac{x^2}{25} + \frac{y^2}{2}\right)},$$

and the coefficients obtained are tabulated in Table I. Also tabulated are the maximum values attained by each term in $F_0(x,y)$. The function $F_0(x,y)$, with these coefficients, was taken as the velocity probability surface to be used throughout the present analysis.

III Dispersions to be Removed from the Velocity Probability Surface

1. Dispersion due to Instrumental Errors

Stein finds that the time resolution of the time-of-flight apparatus is Gaussian with a full width at half maximum of 5.5×10^{-9} sec. Thus the dispersion in the true time t is given by

$$T(t_0-t) = \frac{1}{\sqrt{2\pi}\sigma} e^{-\frac{1}{2}\left(\frac{t_0-t}{\sigma}\right)^2},$$

where t_0 is the observed time and $\sigma = 2.33 \times 10^{-9}$ sec. The velocity v is given by d/t , where $d (= 269 \text{ cm})$ is the distance travelled by the fragment. The dispersion in v is given by

$$\begin{aligned} V(v_0-v) &= T[t(v)] \left| \frac{dt(v)}{dv} \right| \\ &= \frac{d}{\sqrt{2\pi}\sigma} \frac{1}{v^2} e^{-\frac{1}{2}\left(\frac{t_0-d/v}{\sigma}\right)^2}. \end{aligned}$$

The times of flight t lie in the range $1.7 \times 10^{-7} \leq t \leq 3.4 \times 10^{-7}$ sec, and hence $\sigma \ll t$. Therefore $V(v_0-v)$ is very nearly a Gaussian which maximizes at $v = d/t_0$, and so to a very good approximation one can use

$$V(v_0-v) = \frac{1}{\sqrt{2\pi} \sigma_t} e^{-\frac{1}{2} \left(\frac{v_0-v}{\sigma_t} \right)^2},$$

where $\sigma_t = 0.865 \times 10^{-11} v^2$ when v is in units of cm/sec.

2. Dispersion due to Neutron Emission

Fraser and Milton (1958) have calculated the probability density function for the change in the component, along a given axis, of the fission fragment velocity due to the emission of one neutron. They assumed that the angular distribution of neutrons in the centre of mass system depends on the second order Legendre polynomial $P_2(\cos \theta)$ according to the probability density function

$$\Theta(\theta) = 1 + C_2 P_2(\cos \theta),$$

and that the energy spectrum of the neutrons in the centre of mass system depends on the nuclear temperature T according to

$$N(\epsilon) = \frac{1}{T^2} \epsilon e^{-\frac{\epsilon}{T}}.$$

In the present work their probability density function for the change in the component of velocity along the drift tube axis due to one neutron emission is used with the following two modifications. It was assumed that the fragments which are observed have emitted neutrons isotropically in the centre of mass system, so that one can take $C_2 = 0$. In typical cases it is possible for a fragment which is initially travelling in the direction of the drift tube axis to emit a neutron perpendicular to its direction of motion, obtain a component of velocity of about 2.5×10^7 cm/sec in this perpendicular direction, and still be detected if approaching the large detector but not if approaching the small detector. This would necessitate a value of C_2 which would yield

a greater probability of neutron emission along the drift tube axis. However, it turns out that the dispersions to be removed are not large, and so the assumption of isotropic neutron emission is a reasonable one. The density function with $C_2 = 0$ was then approximated by a Gaussian. This is a good approximation for the case $C_2 = 0$. One then obtains the density function

$$w(v_0 - v) = \frac{1}{\sqrt{2\pi} \sigma_1} e^{-\frac{1}{2} \left(\frac{v_0 - v}{\sigma_1} \right)^2},$$

where $\sigma_1 = 0.901 \sqrt{2NT}/m$. Here N is the neutron mass and m is the mass of the fragment before emitting the neutron. Both masses are in atomic mass units. In all of the calculations which follow, the actual mass m of the fission fragment was replaced by its atomic mass A , so that a particular mass division in fission is specified by giving the so-called mass ratio $R = A_H/A_L$, which is the ratio of the atomic masses of the heavy and light primary fission fragments. The nuclear temperature T in the expression for σ_1 is in Mev. The value of nuclear temperature selected for the present calculations is $T = 0.59$ Mev. This is the mean value obtained by Terrell (1959) for the excited fission fragments from U^{235} fission. It is based on experimental fission neutron spectra and the experimental average fission fragment kinetic energy per nucleon, and on the assumption that neutron emission is symmetrical about 90° to the direction in which the fission fragments separate. This value is smaller than that usually assumed for fission fragments. The effect of using this nuclear temperature rather than a higher one is discussed in Chapter IX.

In the case that n neutrons are emitted from the fragment, the

standard deviation σ_1 in the density function W is replaced by

$$\sigma_n = 0.901 \sqrt{2NTn/A},$$

where the change from m to A has also been made. The overall average number of neutrons emitted in the thermal neutron fission of U^{235} is 2.46 per fission. If one assumes that half of these are emitted by each fragment in every fission event, one puts $n = 1.23$ in the expression for σ_n . This value for n is only a first approximation but is a reasonable one to make at this stage of the calculation.

3. Total Dispersion to be Removed

The total dispersion to be removed from the velocity probability surface $F_0(x,y)$ was taken as a Gaussian with standard deviation given by

$$\sigma = \sqrt{\sigma_t^2 + \sigma_n^2}.$$

Using the principles of conservation of momentum, $A_H v_H = A_L v_L$, and conservation of mass, $A_H + A_L = 236$ amu, and taking $T = 0.59$ Mev and $n = 1.23$, one finds that the standard deviations for the dispersion to be removed from the heavy and light fragment velocities v_H^0 and v_L^0 , respectively, are

$$\sigma_L = 10^7 \left[0.748 (10^{-9} v_L)^4 + 0.203 \left(1 + \frac{v_L}{v_H} \right)^2 \right]^{\frac{1}{2}}$$

and

$$\sigma_H = 10^7 \left[0.748 (10^{-9} v_H)^4 + 0.203 \left(1 + \frac{v_H}{v_L} \right)^2 \right]^{\frac{1}{2}},$$

where the velocities are in cm/sec. In order to use these expressions one must know the velocities v_H and v_L of the primary fragments before neutron emission rather than the velocities v_H^0 and v_L^0 which are observed experimentally. Since the experimental velocities differ by less than 3% from those before neutron emission, and the dispersions to be removed are only small corrections to the velocity probability surface, the experimental velocities rather than the velocities before neutron emission

were used in the above expressions.

An estimate was made of the range of values taken on by σ_H and σ_L by evaluating them for velocities which are near to the most probable ones, and for their maximum and minimum values in the range of velocities which occur in fission. The results are given in Tables II and III. In order to estimate the effect of removing from the velocity probability surface the constant dispersions of the magnitude just calculated, a cross section of the surface was taken at $v_H^0 = 0.96 \times 10^9$ cm/sec and another at $v_L^0 = 1.41 \times 10^9$ cm/sec. These cross sections are in the region of greatest probabilities. The cross sections were approximated by Gaussians with standard deviations Σ_H and Σ_L for the cross sections with variable velocities v_H^0 and v_L^0 , respectively. In each case the constant dispersions with standard deviations given in Tables II and III were removed to give a Gaussian with standard deviation $S = \sqrt{\Sigma^2 - \sigma^2}$. The quantity $(\Sigma - S)/S$, which is the increase in the height of the new curve over that of the old curve at their maximum values, is also given in these tables.

The magnitude of the dispersion in the heavy fragment velocities is considerably less than that in the light fragment velocities. This is to be expected, first, because the heavier fragments are moving more slowly and their longer time of flight leads to better time resolution, and secondly, because the velocity change when a neutron is emitted from a heavier fragment is less than when emitted from a lighter fragment. In view of the fact that the per cent errors in the velocity probability surface are probably of the same order of magnitude as the dispersion which would be removed from the heavy fragment velocities, it has been

decided to assume that the velocities v_H^0 which occur in the function $F_0(x,y)$ are the velocities v_H before neutron emission. Hence the probability surface $F_0(x,y)$ need only be corrected for the dispersion in the light fragment velocities.

4. Velocity Loss due to Nickel Source Backing

So far no mention has been made of the velocity slowing which occurs when fission fragments pass through the 0.1 mg/cm^2 nickel foil on which the fissile U^{235} is mounted. The correction for this was made by equating the overall average kinetic energy per fission derived from the present data to that determined calorimetrically in another experiment, and is discussed in Chapter V.

IV Removal of Dispersions from Velocity Probability Surface

One has an analytic expression for the velocity probability function $F_0(v_H^0, v_L^0)$ for the observed velocities v_H^0 and v_L^0 , and wishes to find the velocity probability function $F(v_H, v_L)$ for the velocities v_H and v_L which apply before neutron emission.

One can immediately replace v_H^0 by v_H since it has been concluded that the dispersion in the heavy fragment velocities may be neglected. Then one considers v_H fixed and proceeds to remove the dispersion in v_L^0 . The probability density function for the error in v_L is given by

$$E(v_L^0 - v_L) = \frac{1}{\sqrt{2\pi} \sigma_L} e^{-\frac{1}{2} \left(\frac{v_L^0 - v_L}{\sigma_L} \right)^2},$$

where
$$\sigma_L = 10^7 \left[0.748 (10^{-9} v_L^0)^4 + 0.203 \left(1 + \frac{v_L^0}{v_H^0} \right)^2 \right]^{\frac{1}{2}}.$$

The probability functions are related according to

$$F_0(v_H, v_L^0) = \int_{-\infty}^{\infty} E(v_L^0 - v_L) F(v_H, v_L) dv_L,$$

where v_H^0 has been replaced by v_H . Since σ_L is small compared with the spread in the function F_0 and hence with the spread in the function F , the integrand is appreciable only near $v_L = v_L^0$. Hence one expands $F(v_H, v_L)$ in a Taylor series about $v_L = v_L^0$. The integration then reduces to integrals of the form $\int_{-\infty}^{\infty} x^n e^{-x} dx$, and one obtains

$$F_0(v_H, v_L^0) = \sum_{n=0}^{\infty} \frac{\sigma_L^{2n}}{2^{2n} n!} F^{(2n)}(v_H, v_L^0),$$

where

$$F^{(2n)}(v_H, v_L^0) = \left[\frac{d^{2n}}{du^{2n}} F(v_H, u) \right]_{u = v_L^0}.$$

On solving for $F(v_H, v_L^0)$ one obtains

$$F(v_H, v_L^0) = \sum_{n=0}^{\infty} (-1)^n \frac{\sigma_L^{2n}}{2^{2n} n!} F_0^{(2n)}(v_H, v_L^0).$$

Since σ_L is small one obtains the desired function $F(v_H, v_L)$ by replacing v_L^0 by v_L in the function F . Thus

$$F(v_H, v_L) = \sum_{n=0}^{\infty} (-1)^n \frac{\sigma_L^{2n}}{2^{2n} n!} \left[F_0^{(2n)}(v_H, v_L) \right]_{v_L = v_L^0}.$$

The function F_0 used in this formula is $F_0(x, y)$ given in Chapter II, with the transformation between the variables x and y , and v_H^0 and v_L^0 , as given there.

The derivatives which occur in the above expression for $F(v_H, v_L)$ were found analytically and the cross section of the function $F(v_H, v_L)$ along the x axis, which is one of the symmetry axes, was obtained using terms up to and including the eighth derivative of F_0 . The term depending on the second derivative changed the function $F_0(v_H^0, v_L^0)$ in the manner and by the amount expected, that is, by decreasing the spread of $F_0(v_H^0, v_L^0)$ consistent with the value of σ_L . However, the terms

depending on the higher order derivatives altered between large positive and negative values inconsistent with the value of σ_L . This unruly nature of the higher order correction terms is explained as follows. The function $F_0(v_H^0, v_L^0)$ is the sum of two terms, each of which is the product of a polynomial and a Gaussian. The polynomials are used as corrections to give as good a fit as possible to the observed probability surface. However, because of these polynomials, it does not follow that $F_0(v_H^0, v_L^0)$ will yield derivatives which are a good fit to the derivatives of the probability surface. The fact that the erratic behaviour of the higher order correction terms is due to the multiplying polynomials was checked by setting the coefficients of all but the constant term equal to zero. The correction term depending on the second order derivative was of course changed, but the main feature was that all the other correction terms were negligible compared with the first correction term. This procedure not only verifies the effect of the multiplying polynomials but also helps to justify the assumption that the first correction term is the only important one. It was therefore decided to obtain the probability function for the velocities v_H and v_L by using the formula

$$F(v_H, v_L) = \left[F_0(v_H, v_L) - \frac{\sigma_L^2}{2} F_0^{(2)}(v_H, v_L) \right]_{v_L=v_L^0}$$

An illustration of the dispersion removal in the total fission fragment kinetic energy density function for the mass division $R = 143/93$ is given in Figure 1. Reference should be made to Chapter V for details of the calculation of these curves.

V Kinetic Energy Distributions

1. Kinetic Energy Distribution at Constant Mass Ratio

From the velocity probability surface $F(v_H, v_L)$ one can obtain the probability density function for the total kinetic energy E_K of the fragments specified by the mass ratio R . One introduces the polar co-ordinates (r, θ) defined by

$$v_H = r \cos \theta, \quad v_L = r \sin \theta,$$

so that

$$R = \frac{v_H}{v_L} = \tan \theta,$$

and hence fission with a given mass ratio is specified by a constant value of θ . The principles of conservation of momentum, $A_H v_H = A_L v_L$, and conservation of mass, $A_H + A_L = A$, allow one to write the total kinetic energy as

$$E_K = \frac{AR}{2(R^2 + 1)} r^2.$$

With the transformation to polar co-ordinates the probability $F(v_H, v_L) dv_H dv_L$ becomes $F(v_H, v_L) r dr d\theta$, and hence the probability density function for E_K at constant mass ratio is given by

$$\begin{aligned} P'_K(E_K; R) &= F(v_H, v_L) r \frac{dr}{dE_K} \\ &= \frac{R^2+1}{AR} F\left(\sqrt{\frac{2E_K}{AR}}, \sqrt{\frac{2RE_K}{A}}\right). \end{aligned}$$

It is observed that each of these kinetic energy distributions is simply a cross section of the velocity probability surface weighted by a factor depending on the mass ratio.

2. Adjustment of Velocities to Yield Calorimetric Average Kinetic Energy

A correction was now made to the velocities v_H and v_L for the fission fragment velocity loss which occurs for fragments which pass through the nickel foil on which the fissile material is mounted. To

do this, the overall average kinetic energy of the fragments per fission obtained from the probability surface $F(v_L, v_H)$ has been fitted to that determined calorimetrically by Leachman and Schafer (1955). Their value of 167.1 ± 1.6 Mev for the overall average kinetic energy of the fragments per fission was used to make the correction. The correction was made on the assumption that the velocity of each fragment is reduced by 100q% in the nickel foil, where the constant q is to be determined. The assumption of the same per cent loss for all velocities is justified on the basis that the velocity loss is small. It might be noted that this assumption leads to the velocity bunching observed by Leachman and Schmitt (1954) in their investigation of the slowing of fission fragments in thick foils.

Let E_K^t , v_H^t , and v_L^t be the true values for the total kinetic energy, heavy fragment velocity, and light fragment velocity, respectively, before neutron emission and before the fragments have been slowed down. As previously, E_K , v_H , and v_L are the same quantities before the slowing down correction has been made. Let $P_K^t(E_K^t; R)$ be the probability density function for E_K^t , and, as before, let $P_K(E_K; R)$ be that for E_K . Then the overall average kinetic energy of the fragments per fission before velocity loss occurs is given by

$$\langle E_K^t \rangle = \frac{\sum_R \int E_K^t P_K^t(E_K^t; R) dE_K^t}{\sum_R \int P_K^t(E_K^t; R) dE_K^t},$$

where the integrals and sums are taken over all energies and mass ratios, respectively, for which the probability density function is appreciable. Using the principles of conservation of momentum, $A_H v_H^t = A_L v_L^t$, and of mass, $A_H + A_L = 236$, one obtains

$$E_K^t = 118 v_H^t v_L^t .$$

Similarly, the overall average kinetic energy of the fission fragments per fission as calculated from the known function $P_K(E_K; R)$ is given by

$$\langle E_K \rangle = \frac{\sum_R \int E_K P_K(E_K; R) dE_K}{\sum_R \int P_K(E_K; R) dE_K} ,$$

where

$$E_K = 118 v_H v_L .$$

The assumption regarding the overall average kinetic energy requires that

$$\langle E_K^t \rangle = 167.1 \text{ Mev} ,$$

and the assumption of a 100q% velocity loss requires that

$$v_H = v_H^t (1-q),$$

$$\text{and } v_L = v_L^t (1-q).$$

When one uses these assumptions and the relationship

$$P_K^t(E_K^t; R) = P_K(E_K; R)$$

between the probability density functions, one obtains

$$\langle E_K \rangle = 167.1 (1-q)^2,$$

and hence q can be obtained.

The integrations involved in calculating $\langle E_K \rangle$ were performed numerically using the trapezoidal rule, and the average kinetic energy \bar{E}_K at each mass ratio was obtained. The sum was then taken over all mass ratios, and the overall average kinetic energy $\langle E_K \rangle = 164.8 \text{ Mev}$ was obtained. This is consistent with the value of $165 \pm 2 \text{ Mev}$ obtained by Stein from the same data. From the value of $\langle E_K \rangle$ calculated in the present work one finds $q = 0.0069$, which corresponds to a 0.69% velocity loss in the nickel foil. This means that all energies must now be increased by 1.38%. The resulting true average kinetic energies $\bar{E}_K^t = \bar{E}_K / (1-q)^2$ at a given mass ratio are plotted in Figure 5 for those mass

divisions for which the primary fragments have odd mass numbers.

In order to take the fragment velocity loss into account in all subsequent evaluations which use the kinetic energy probability density function $P_K(E_K; R)$, one replaces v_H , v_L , and E_K where they occur by $v_H^t(1-q)$, $v_L^t(1-q)$, and $E_K^t(1-q)^2$, respectively, so that the function $P_K(E_K; R)$ becomes a function depending on the true velocities which apply before neutron emission and slowing down in the foil occur. One therefore takes

$$P_K(E_K; R) \equiv P_K \left[E_K^t(1-q)^2; R \right] .$$

3. Example of Dispersion Removal in Kinetic Energy Distributions

An example of the effect of removing the neutron emission and instrumental dispersions from the kinetic energy probability density function for the mass division $R = 143/93$ is given in Figure 1. The functions plotted are (a), the kinetic energy probability density function which has been corrected for the velocity loss in the nickel foil and for the neutron emission and instrumental dispersions, and (b), the kinetic energy probability density function which has been corrected for only the velocity loss in the nickel foil. The former function is

$$P_K \left[E_K^t(1-q)^2; R \right] = \frac{R^2+1}{AR} F \left(\sqrt{\frac{2 E_K^t(1-q)^2}{AR}}, \sqrt{\frac{2R E_K^t(1-q)^2}{A}} \right)$$

and the latter is the same function with $\sigma_L = 0$.

4. Simplified Analytic Form for Certain Kinetic Energy Distributions

The analytic form of the kinetic energy probability density function $P_K \left[E_K^t(1-q)^2; R \right]$ is quite complicated, and so, in order to reduce the computation time required in the use of this function in subsequent work, the function was approximated for certain mass ratios

by one of simpler analytic form. These are all the mass ratios involving primary fission fragments of odd mass number for which the probability of fission is greater than 4% of that for the most probable mass division. These are fourteen mass ratios in the range $R = 1.17$ to $R = 1.84$. The function P_K was approximated by

$$Q_K(E_K^t; R) = A_1 e^{-\frac{1}{2}\left(\frac{E_K^t - E_1}{\sigma_1}\right)^2} + A_2 e^{-\frac{1}{2}\left(\frac{E_K^t - E_2}{\sigma_2}\right)^2},$$

where E_1 , E_2 , σ_1 , and σ_2 were chosen on the basis of graphs of the function P_K , and the coefficients A_1 and A_2 were determined by the method of least squares. In all cases the proper choice of the means and standard deviations assured that the function Q_K differed negligibly from the function P_K . The functions Q_K so obtained are plotted in Figures 3, 4, and 5, and the constants used in their evaluation are given in Table IV.

VI Total Energy Release in Fission

1. Total Energy Release in a Particular Fission Mode

From the conservation of energy equation given in the Introduction the total energy release in the thermal neutron fission of U^{235} is given by

$$E_T = \left[M(235, 92) + N \right] - \left[M_H(A_H, Z_H) + M_L(A_L, Z_L) \right],$$

where $A_H + A_L = 236$ and $Z_H + Z_L = 92$. The neutron mass N was taken to be 1.00898 amu. The unknown primary fragment masses M_H and M_L were taken from the mass table compiled by Cameron (1957). His mass formula includes volume, surface, coulomb, and coulomb exchange energies, and also empirically determined shell correction and pairing energies. The

measured masses used in his formula are taken from the tables of Wapstra (1955) and Huizenga (1955).

Particular attention was given to the choice of the mass $M(235,92)$ of the U^{235} nuclide. Wapstra (1955) gives this mass as 235.117496 ± 140 amu. More recently, Duckworth (1957) has published a table of atomic masses which gives the U^{235} mass as 235.116600 ± 500 amu, which is based on the value 208.040700 ± 500 amu for the mass of Pb^{208} . The precision measurements of Demirkhanov, Gutkin, and Dorokhov (1959) indicate that a better value for the mass of lead is 208.042658 ± 35 amu. When this value for the mass of Pb^{208} is inserted in Duckworth's calculations, one obtains the U^{235} mass as 235.118558 ± 500 amu. This value, which is about one Mev greater than that given by Wapstra, is the value which was used in calculations of the total energy release E_T .

2. Charge Distribution for a Given Mass Ratio

Corresponding to the mass division specified by the mass ratio R there are many possible charge divisions, each with a different total energy release. The most probable charge division for the mass ratio R was determined on the assumption that this is the charge division which gives the greatest total energy release. This hypothesis was used by Kennett and Thode (1956) and successfully explained their independent fission yield measurements for I^{128} . The distribution about the most probable charge was based on the work of Cohen and Fulmer (1958). By putting gas into a magnetic spectrometer they achieved a mass separation of the fission fragments, and from the width of the distribution for a given fragment mass they found that

the full width at half maximum of the nuclear charge distribution is 2.4 ± 0.5 charge units for most masses. This is the value which was used in the present work. Hence the charge distribution for a given mass ratio was obtained by using the maximum energy release hypothesis to determine the most probable charge division and by using a Gaussian with full width at half maximum of 2.4 charge units to obtain the charge distribution. The peak of the Gaussian was located either at the charge division which gave the greatest energy release or half way between two charge divisions which gave comparable greatest energy releases.

3. Mean Total Energy Releases for a Given Mass Ratio

For each mass ratio R for which kinetic energy distributions have been plotted in Figures 2, 3, and 4, the total energy release E_T was calculated for various possible charge divisions, and the mean total energy release \bar{E}_T for each mass ratio was obtained using weight factors from the Gaussian distribution described in the preceding section. These mean energies \bar{E}_T are plotted in Figure 5 along with the mean kinetic energies \bar{E}_K^t which were obtained as described in Chapter V. Also plotted are the mean excitation energies given by

$$\bar{E}_X^t = \bar{E}_T - \bar{E}_K^t.$$

It is of interest to point out that the mean total energy releases \bar{E}_T were also calculated from the mass table of Hay and Newton (1956) which was first altered to the new U^{235} mass of 235.118558 ± 500 amu. Since the energy releases from this altered mass table are in many cases from 3 to 6 Mev greater than those calculated from Cameron's table, the resulting mean total energy releases are greater than Cameron's by about the same amount. The importance of this

difference in the excitation energies of the fission fragments is appreciable in view of the fact that the excitation energies, being differences between two large energies, are greatly influenced by even small per cent errors in the total energy release. An attempt was made to replace some of the masses of Wapstra (1955), which were used as the measured masses for the table of Hay and Newton, by those which are presented by Duckworth (1957). In a few cases total energy releases were reduced by 0.5 to 1 Mev, but there was no consistent energy reduction.

VII Single Fragment Excitation Energy Distributions

The normalized total excitation energy probability density function obtained from the total kinetic energy probability density function $Q_K(E_K^t; R)$ is given at each mass ratio by

$$Q_X(E_X^t; R) = \frac{1}{\sqrt{2\pi}(\sigma_1 A_1 + \sigma_2 A_2)} \left\{ A_1 e^{-\frac{1}{2} \left[\frac{(E_T - E_1) - E_X^t}{\sigma_1} \right]^2} + A_2 e^{-\frac{1}{2} \left[\frac{(E_T - E_2) - E_X^t}{\sigma_2} \right]^2} \right\},$$

where the relationship $E_K^t + E_X^t = E_T$ has been used, and the total energy release E_T is obtained as described in Chapter VI. The other constants which appear in the above function are given in Table IV.

As stated in the Introduction, there is no fundamental principle which one might use to determine the division of this total excitation energy between the two fragments. However, on the assumption that the fraction r , $0 \leq r \leq 1$, of the total excitation energy is given to the light fragment, the light fragment excitation energy E_{XL}^t has a normalized probability density function given by

$$Q_{XL}(E_{XL}^t; R, r) = \frac{1}{r\sqrt{2\pi}(\sigma_1 A_1 + \sigma_2 A_2)} \left\{ A_1 e^{-\frac{1}{2} \left[\frac{r(E_T - E_1) - E_{XL}^t}{r\sigma_1} \right]^2} + A_2 e^{-\frac{1}{2} \left[\frac{r(E_T - E_2) - E_{XL}^t}{r\sigma_2} \right]^2} \right\}$$

and similarly for the heavy fragment which receives the fraction $(1-r)$ of the total excitation energy.

VIII Conditional Neutron Emission Probabilities

Following the method of Blatt and Weisskopf (1952), the probabilities that a fission fragment with excitation energy E will emit exactly n neutrons were derived for excitation energies for which up to four neutrons can be emitted. These conditional neutron emission probabilities are denoted by $p(n; \beta_{s-1} \leq E \leq \beta_s)$, where this is the probability that exactly n neutrons are emitted by a fragment with excitation energy E , and where the range of the excitation energy for which the expression is valid is given explicitly. The definition

$$\beta_s = \sum_{i=1}^s B_i$$

has been used, where B_i is the separation energy of the i th neutron.

In the derivation of these probabilities it was assumed that the kinetic energy ϵ of the neutron has a probability density function given by

$$N(\epsilon) = \frac{\epsilon}{T^2} e^{-\frac{\epsilon}{T}},$$

where T is the nuclear temperature. It was also assumed that neutrons are always emitted when emission is energetically possible. This means, for example, that $p(1; \beta_1 \leq E \leq \beta_2) = 1$, and $p(n; \beta_1 \leq E \leq \beta_2) = 0$ for $n \neq 1$. Since it was found that the probability $p(1; \beta_3 \leq E \leq \beta_5)$ is negligible, this probability was taken to be zero. Also, advantage was taken of the fact that the sum of the probabilities within each energy range must be unity.

The following are the conditional neutron emission probabilities derived on these assumptions.

$$p(0; 0 \leq E \leq \beta_1) = 1$$

$$p(1; \beta_1 \leq E \leq \beta_2) = 1$$

$$p(1; \beta_2 \leq E \leq \beta_3) = 1 - p(2; \beta_2 \leq E \leq \beta_3)$$

$$p(2; \beta_2 \leq E \leq \beta_3) = \frac{1 - \left(1 + \frac{E - \beta_2}{T}\right) e^{-\frac{E - \beta_2}{T}}}{1 - \left(1 + \frac{E - \beta_1}{T}\right) e^{-\frac{E - \beta_1}{T}}}$$

$$p(2; \beta_3 \leq E \leq \beta_4) = 1 - p(3; \beta_3 \leq E \leq \beta_4)$$

$$p(3; \beta_3 \leq E \leq \beta_4) = 1 - \left[1 + \left(\frac{E - \beta_3}{T}\right) + \frac{1}{2}\left(\frac{E - \beta_3}{T}\right)^2 + \frac{1}{6}\left(\frac{E - \beta_3}{T}\right)^3\right] e^{-\frac{E - \beta_3}{T}}$$

$$p(2; \beta_4 \leq E \leq \beta_5) = \left[\left(1 + \frac{E - \beta_3}{T}\right) e^{-\frac{E - \beta_3}{T}} - \left(1 + \frac{E - \beta_2}{T}\right) e^{-\frac{E - \beta_2}{T}}\right] \left[1 + \frac{1}{2}\left(\frac{E - \beta_3}{T}\right)^2\right] - \left[\frac{1}{3} e^{-\frac{E - \beta_3}{T}} - e^{-\frac{E - \beta_2}{T}}\right] \left[\frac{E - \beta_3}{T}\right]^3$$

$$p(3; \beta_4 \leq E \leq \beta_5) = 1 - p(2; \beta_4 \leq E \leq \beta_5) - p(4; \beta_4 \leq E \leq \beta_5)$$

$$p(4; \beta_4 \leq E \leq \beta_5) = 1 - \left[1 + \left(\frac{E - \beta_4}{T}\right) + \frac{1}{2}\left(\frac{E - \beta_4}{T}\right)^2 + \frac{1}{6}\left(\frac{E - \beta_4}{T}\right)^3 + \frac{1}{24}\left(\frac{E - \beta_4}{T}\right)^4 + \frac{1}{120}\left(\frac{E - \beta_4}{T}\right)^5\right] e^{-\frac{E - \beta_4}{T}}$$

The derivation for the probability $p(3; \beta_3 \leq E \leq \beta_4)$ is now given.

The energy diagram for this case is shown in Figure 6. The original fragment of mass number A has an excitation energy E above its

ground state energy represented by the solid horizontal line labelled with an A. The excitation energy E lies in the range $\beta_3 \leq E \leq \beta_4$. The minimum excitation energy required to emit the first neutron is B_1 , and so the ground state energy of the fragment A-1 is displaced from that of fragment A by an energy B_1 . The other ground state energies are similarly drawn.

The first neutron is emitted with kinetic energy ϵ , and the fragment A-1 is left with excitation energy $E' = E - B_1 - \epsilon$. Clearly one must have $0 \leq \epsilon \leq E - \beta_2$ for a second neutron to be emitted, and $0 \leq \epsilon \leq E - \beta_3$ if there is to be a possibility for the emission of a third neutron. However, if $0 \leq \epsilon \leq E - \beta_3$, either two or three neutrons may be emitted. Three neutrons will be emitted if, given $0 \leq \epsilon \leq E - \beta_3$, the kinetic energy ϵ' of the second neutron lies in the range $0 \leq \epsilon' \leq E' - B_2 - B_3$, that is, in the range $0 \leq \epsilon' \leq E - \beta_3 - \epsilon$. This probability is given by

$$M(\epsilon) = \frac{\int_0^{E-\beta_3-\epsilon} N(\epsilon') d\epsilon'}{\int_0^{E-\beta_2-\epsilon} N(\epsilon') d\epsilon'} ,$$

and the probability of emitting three neutrons is given by

$$p(3; \beta_3 \leq E \leq \beta_4) = \frac{\int_0^{E-\beta_3} N(\epsilon) M(\epsilon) d\epsilon}{\int_0^{E-\beta_1} N(\epsilon) d\epsilon} .$$

It turns out that for the neutron separation energies to be used the integrals

$$\int_0^{E-\beta_1} N(\epsilon) d\epsilon \quad \text{and} \quad \int_0^{E-\beta_2-\epsilon} N(\epsilon') d\epsilon'$$

may be set equal to unity. This is an underestimation of the value of the first integral by a negligible amount. For a nuclear temperature $T = 0.59$ Mev it is at worst an underestimation of value of the second integral by 0.7%, and the average underestimation is less than 0.01%. Similar approximations were used in deriving some of the other conditional neutron emission probabilities.

IX Neutron Emission Calculations

1. Method of Calculation

Using the single fragment excitation energy probability density functions $Q_{XL}(E_{XL}^t; R, r)$ given in Chapter VII and the conditional neutron emission probabilities $p(n; \beta_{s-1} \leq E_{XL}^t \leq \beta_s)$ given in Chapter VIII, one can calculate the number of neutrons emitted by the light fragment when its excitation energy is in the range specified. This is given by

$$n_L(\beta_{s-1} \leq E_{XL}^t \leq \beta_s) = \int_{\beta_{s-1}}^{\beta_s} p(n; \beta_{s-1} \leq E_{XL}^t \leq \beta_s) Q_{XL}(E_{XL}^t; R, r) dE_{XL}^t.$$

When the integrals of the above form are evaluated for the entire range of excitation energies and the results are added together, one obtains the number n_L of neutrons emitted by the light fragment. Similarly one can obtain the number n_H of neutrons emitted by the heavy fragment, and hence the total number $n = n_L + n_H$ emitted in the fission mode specified by the mass ratio R and excitation energy division r . The various cases in which the above integrals were evaluated are discussed in the following sections. All evaluations were done numerically using the trapezoidal rule with excitation energy intervals of 0.1 Mev.

2. Parameters Involved in the Calculations

The quantities which must be fixed in the conditional neutron emission probabilities before evaluations can proceed are the separation energies B_1 and the nuclear temperature T . The neutron separation energies were taken from the mass tables derived by Cameron (1957). However, in the final calculations the mean separation energies defined in the following section were used. The nuclear temperature was assumed to have the constant value of 0.59 Mev calculated for fission fragments by Terrell (1959) and which has already been used in the present work when the neutron emission dispersion was removed from the velocity probability surface. The effect of using a higher nuclear temperature was investigated and is discussed in Section 4 of this chapter.

The quantities which remain to be fixed in the single fragment excitation energy density function are the total energy release E_T and the fraction r of the total excitation energy which goes to the light fragment. The values for E_T are taken from the mass table derived by Cameron (1957) which was altered to take into account the new U^{235} mass in the manner described in Chapter VI. However, the final calculations were performed using the mean energies \bar{E}_T which were defined in the same chapter. This is discussed in the following section. As for the parameter r , in most cases it was assumed to be 0.5, but variations from this value were also considered and are discussed in Section 5 of this chapter.

In the following sections the effect of varying the parameters just discussed is considered for the fission mode specified by the mass ratio $R = 143/93$.

3. Mean Values for Separation Energies and Total Energy Release

Although for one mass division specified by the mass ratio R there are many possible charge divisions each of which gives rise to a different total kinetic energy distribution, the present calculations yield only one kinetic energy distribution for each mass ratio. Since the kinetic energy is derived mainly from the Coulomb repulsion of the two fission fragments, one might expect that the mean kinetic energy for each charge division is closely proportional to the product of the nuclear charges. For the mass ratio $R = 143/93$ the mean kinetic energy was found to be $\bar{E}_K = 163.06$ Mev. Table V gives the mean kinetic energies $\bar{E}_K(Z_H, Z_L)$ derived on the above basis for the charge divisions which are reasonably probable. The defining equation used was

$$\bar{E}_K = \sum w \bar{E}_K(Z_H, Z_L),$$

where

$$\bar{E}_K(Z_H, Z_L) \propto Z_H Z_L.$$

The weight factors w were taken from the Gaussian charge distribution discussed in Chapter VI. The corresponding total energy releases and Separation energies are also given. With each mean total energy release $\bar{E}_K(Z_H, Z_L)$ was associated a kinetic energy distribution which had this value for its mean and a shape identical with that of the original distribution for the mass ratio $R = 143/93$. Using these kinetic energy distributions, an equal division of total excitation energy between the two fragments, and a nuclear temperature of 0.59 Mev, the number of neutrons emitted was calculated for each case. The weighted number of neutrons emitted was found to be $n_L = 1.42$ from the light fragment and $n_H = 1.79$ from the heavy, giving a total of $n = 3.21$ neutrons.

The question of whether the number of neutrons emitted in

fission with the mass ratio $R = 143/93$ could be obtained by a shorter method was then investigated. One calculation was performed using the original kinetic energy distribution with mean kinetic energy $\bar{E}_K = 163.06$ Mev, mean separation energies, and a mean total energy release. For each i the mean separation energy \bar{B}_i was obtained by using the same weight factors w as have already been used. The total energy releases of the previous calculations were weighted with the factors w to obtain the mean total energy release. The results for n_L , n_H , and n were 1.39, 1.81, and 3.20 neutrons, respectively. The single fragment excitation energy distributions and the conditional neutron emission probabilities used in this calculation are plotted in Figures 7 and 8.

The agreement between the results of this approximate calculation and the previous one is remarkable. In fact, whenever B_3 or B_4 are below about 4 Mev the approximations used in determining certain of the conditional neutron emission probabilities are not satisfactory and the results so obtained are expected to be slightly low. In any case, it seems reasonable to use mean separation energies and a mean total energy release, as well as the average kinetic energy distribution which has previously been derived. This is what was done in all the remaining calculations.

4. Dependence of Neutron Emission on Nuclear Temperature

The nuclear temperature used in the calculations of the previous section was the value $T = 0.59$ Mev obtained by Terrell (1959) as the mean value for the thermal neutron fission of U^{235} . In contrast, a nuclear temperature of 1.40 Mev was used by Leachman (1956) and Leachman and Kazek (1957) in the calculation of neutron emission probabilities

from ionization chamber data. This latter value was obtained by fitting the neutron energy distribution $N(\epsilon) = \frac{\epsilon}{T^2} e^{-\epsilon/T}$ to measured (n, 2n) excitation functions. In order to check the dependence of neutron emission on the nuclear temperature, the final calculation of the previous section, that using average energies and an equal division of excitation energy between the fragments, was repeated using a nuclear temperature of 1.00 Mev. The results for n_L , n_H , and n are 1.31, 1.66, and 2.97 neutrons, respectively, as given in Table VI. The single fragment excitation energy distributions and the conditional neutron emission probabilities are plotted with those for $T = 0.59$ in Figures 7 and 8. These results might mean that the nuclear temperature should be increased, since the increased nuclear temperature gives closer agreement between the calculated number of neutrons emitted from the fission mode $R = 143/93$ and the experimental average over all modes of 2.46 per fission. However, in order to investigate other dependences, the nuclear temperature was kept at 0.59 Mev for all the remaining calculations.

It might be well to point out that the nuclear temperature has occurred in the dispersion, due to neutron emission, which was removed from the velocity surface. There the value $T = 0.59$ Mev was used. Since the dispersion removed was small, the total kinetic energy distributions $Q_K(E_K^t; R)$ are increased by only about 2% at their maximum value when the temperature $T = 1.00$ is used. Hence the larger value of T does not affect the total excitation energy distributions sufficiently to produce a noticeable change in the number of neutrons emitted. In fact, the width of the excitation energy distribution would have to be decreased considerably to change the number of neutrons emitted, because as well as

decreasing the probability of emitting 2 or 3 neutrons at energies greater than 10 Mev, say, it also decreases the probability of emitting 0 or 1 neutron at energies less than 10 Mev. Whether this would result in an increase or decrease in the neutron emission would then depend on the neutron separation energies involved. The general conclusion is that the number of neutrons emitted is not a sensitive function of the shape of the excitation energy distribution, and hence is not a sensitive function of the nuclear temperature which is used in the dispersion removal procedure.

5. Dependence of Neutron Emission on Division of Total Excitation Energy between Fragments

The dependence of the neutron emission on the fraction r of the total excitation energy given to the light fragment was investigated for the mass ratio $R = 143/93$. Mean separation and total energies were used, and the nuclear temperature was taken to be 0.59 Mev. The number of neutrons emitted was calculated for the fractions $r = 0.4, 0.6, \text{ and } 0.7$, and the results are compared in Table VII with those for the fraction $r = 0.5$ which has already been calculated. The overall decrease in n with increasing r is a result of the fact that the heavy fragment separation energies are less than the light fragment separation energies. Therefore the increase in the number of neutrons emitted by the light fragment when its excitation energy is increased is more than compensated for by the decrease in the number of neutrons emitted by the heavy fragment. The dramatic change in the values of n_L and n_H with r is of course expected. However, without further information it is impossible to select a reasonable value for r other than $r = 0.5$. Limited experimental

information is available and is presented in Chapter X.

6. Dependence of Neutron Emission on Mean Total Energy Release

The dependence of the number of neutrons emitted on the mean total energy release \bar{E}_T was investigated for the mass ratio $R = 143/93$. Using mean separation energies, $T = 0.59$ Mev, and $r = 0.5$, the mean total energy release \bar{E}_T was altered in three separate calculations by the amounts $\Delta\bar{E}_T = -1.5, -3.0, \text{ and } -4.5$ Mev. The results are given in Table VIII and show that a decrease by a few Mev has a considerable effect on the number of neutrons emitted.

A number of considerations might justify the inclusion of a negative $\Delta\bar{E}_T$ in the calculations. The values taken for the primary fragment masses in determining the total energy release could easily be in error in the direction which would require a negative $\Delta\bar{E}_T$. Another possibility is that the charge distribution for a given mass ratio assumed in Chapter VI has too small a spread. An increase in the full width at half maximum from 2.4 charge units, which was used from the experimental value of 2.4 ± 0.5 , to 3.0 charge units has the effect of reducing the total energy release for the mode $R = 143/93$ by about 0.8 Mev. Still another possibility is that the maximum energy release hypothesis is not strictly valid. If the most probable charge division for the mode $R = 143/93$ were displaced by only one charge unit from that which has been used in the previous calculations, the mean total energy release would be reduced by about 2 Mev. Hence the proper value for the mean total energy release \bar{E}_T is uncertain by an amount which could reduce the number of neutrons emitted in this mode to a value close to the overall average.

7. Neutron Emission Calculations for Fourteen Mass Ratios

The calculations of the numbers of neutrons emitted were extended to include the mass ratios for which the primary fragments have odd mass numbers and the probability of fission is greater than 4% of that for the most probable mass division. These are the fourteen mass ratios for which the kinetic energy distributions have been plotted in Figures 3, 4, and 5. The fraction of the total excitation energy going to the light fragment was taken to be $r = 0.5$, and the nuclear temperature was taken to be $T = 0.59$ Mev. Mean separation energies and the kinetic energy distributions of Figures 3, 4 and 5 were used. The calculations were performed for two sets of mean total energy releases. The first set consisted of the energies \bar{E}_T calculated by the method of Chapter VI and plotted in Figure 5. The results of the calculation are plotted in Figure 9. The second set of mean total energy releases consisted of those of the first set each of which was altered by the energy $\Delta\bar{E}_T = -3.0$ Mev. Whereas the first set gave the averages $\bar{n}_L = 1.34$, $\bar{n}_H = 1.61$, and $\bar{n} = 2.95$ neutrons per fission when weighted by the fission probabilities of Figure 5, the second set gave the averages $\bar{n}_L = 1.14$, $\bar{n}_H = 1.37$, and $\bar{n} = 2.51$ neutrons per fission. This illustrates the sensitivity of neutron emission to the value assumed for the total energy release.

X Discussion of Neutron Emission Calculations

1. Comparison of Calculations with Experimental Determinations

The experimental information regarding the emission of neutrons from various fission modes is limited. Fraser and Milton (1954) have used ionization chamber techniques to study the neutron emission from individual fragments as a function of mass ratio for the thermal neutron

fission of U^{233} . They find that the neutrons are emitted in nearly equal numbers by each fragment for mass ratios near the most probable fission mode, that neutron emission by the lighter fragment predominates at lower mass ratios, and that neutron emission by the heavier fragment predominates at higher mass ratios. At low mass ratios where fission can still be observed with reasonable probability, the light fragment emits about three times as many neutrons as the heavy fragment, and the reverse is true at high mass ratios. They also observe that the total number of neutrons emitted is approximately constant in the region of mass ratios which contains the majority of the fission events, and that in the overall process the light fragment emits about 30% more neutrons than the heavy fragment. Whetstone (1959) has used time-of-flight techniques and a liquid scintillator neutron detector to study the neutron emission from individual fragments as a function of mass ratio for the spontaneous fission of Cf^{252} . He observes predominant neutron emission by the light fragment at low mass ratios and predominant neutron emission by the heavy fragment at high mass ratios similar to the observations with U^{233} . However, the total number of neutrons emitted decreases as the mass ratio increases, and in the overall process the light and heavy fragments emit approximately equal numbers of neutrons.

A preferential neutron emission by the light fragment at low mass ratios and by the heavy fragment at high mass ratios is evident in the calculations shown in Figure 9. Since at each mass ratio an equal division of the total excitation energy has been assumed, the neutron separation energies of the two fragments determine which fragment emits the greater number of neutrons. Since the general trend in separation

energies is a decrease with increasing fragment mass number, neutron emission from the heavy fragment increases with increasing mass ratio. However, Figure 9 shows that the effect of the separation energies alone is not sufficient to produce the dramatic predominances in the experimentally observed neutron emission. These experimental neutron emission characteristics at low and high mass ratios are best accounted for by assuming an unequal division of the total excitation energy between the primary fission fragments. At low mass ratios the light fragment receives more excitation energy than the heavy fragment, and at high mass ratios the situation is reversed. Table VII, whose derivation has already been described, gives the dependence of neutron emission on the fraction of the excitation energy which is given to the light fragment. From this table one can predict that at the low mass ratios shown in Figure 9 about 70% of the total excitation energy is given to the light fragment, and at the high mass ratios shown in Figure 9 about 35% of the total excitation energy is given to the light fragment. At intermediate mass ratios the excitation energy division lies between these limits.

The variation of the total number of neutrons emitted as a function of mass ratio as plotted in Figure 9 shows the expected similarity to the variation of the mean total excitation energies plotted in Figure 5. Variations in the neutron separation energies with mass ratio account for the slight departures from exact similarity of the two curves.

As has already been stated, the data plotted in Figure 9 yield 2.95 neutrons as the overall average number of neutrons per fission. Here one has assumed $r = 0.5$, $T = 0.59$ Mev, and $\Delta\bar{E}_T = 0$. In view of the

fact that the excitation energy fraction r should not be assumed the same for all mass ratios, that the proper value for the nuclear temperature is in doubt, and that the mean total energy releases \bar{E}_T are only approximate, this value for the average number of neutrons per fission is as close to the experimental value of 2.46 neutrons per fission as can be expected. As has been shown, the calculated average number of neutrons per fission can be reduced to approximately the experimental value by using the parameters $r = 0.5$, $T = 0.59$ Mev, and $\Delta\bar{E}_T = -3.0$ Mev. From the neutron emission dependence on the nuclear temperature as shown in Table VI, one can predict that the parameters $r = 0.5$, $T \approx 1.40$ Mev, and $\Delta\bar{E}_T = 0$ would also bring the calculated average number of neutrons per fission in agreement with the experimental value. As discussed in Chapter IX, Section 4, this is the nuclear temperature used in the calculations of neutron emission done by Leachman (1956) and Leachman and Kazek (1957).

2. Cumulative Yield Curves

It should be kept in mind that a fundamental assumption underlying the neutron emission calculations is that the velocity probability surface can be approximated by a function whose cross sections along two perpendicular axes are essentially Gaussian. In view of the limited experimental data this was a reasonable assumption, but it has the effect of hiding any irregular variations with mass ratio. Also, in removing the neutron emission dispersion from the velocity probability surface it was assumed that each fragment emits exactly half the overall average number of neutrons emitted per fission, and this neglects the known neutron emission variations with fragment mass. Therefore the primary yield curve which is plotted in Figures 5 and 9 is only an

approximation to the true primary yield curve. In principle it would be possible to use this approximate primary yield curve and the neutron emission probabilities calculated in the present work to derive a cumulative yield curve which would give the distribution of mass numbers of the fragments after neutron emission. This might then be compared with the cumulative yield curves which have been determined radiochemically. However, because of the approximate nature of the primary yield curve which has been derived and because of the uncertain values for the parameters in the neutron emission calculations, this has not been done.

3. Conclusions

The neutron emission calculations for each mass division depend critically on two considerations. The first is the value used for the mean total energy release. In establishing the total energy release for a given mass and charge division one must use fragment masses which are determined from a semi-empirical mass formula and the mass of the U^{235} nucleus which is determined indirectly from measurements of the mass of Pb^{208} . In addition, since time-of-flight data give no information concerning the charge distribution for a given mass ratio, an assumption must be made about the charge distribution for a given mass distribution. The resulting mean total energy releases may therefore be in error by energies of the order of several Mev. Table VIII shows that the total number of neutrons per fission emitted from a fission fragment near the most probable mass division may be reduced by 0.47 neutrons when the total energy release is reduced by 3 Mev. This illustrates the sensitivity of the calculations to the value of the

mean total energy release used for a given mass division.

The second important consideration which critically affects the neutron emission calculations for a given mass division is the division of the total excitation energy between the two fission fragments. The evidence for how this energy is divided is taken from experimental data which give the number of neutrons emitted from specific fission fragments. In order to calculate the single fragment neutron emission which corresponds to this experimental data, one must specify that about 70% of the total excitation energy must be given to the light fragment for low mass ratios, that about 35% must be given to the light fragment at high mass ratios, and that the excitation energy given to the light fragment must lie between these limits in the intermediate region of mass ratios where fission is most probable.

The correction for fragment velocity loss in the nickel foil has a considerable effect on the neutron emission calculations. Each velocity was increased by 0.69%, and this increased the time-of-flight overall average kinetic energy of the fragments per fission from 164.8 Mev to the calorimetric value of 167.1 Mev. From Table VIII one sees that this increase of 2.3 Mev means that the calculated number of neutrons emitted from each fragment pair for fission near the most probable mass division is about 0.4 neutrons per fission less than the number which would be emitted if this correction had not been made. This shows the importance of this velocity correction. It is of course possible that the true average kinetic energy of the fragments per fission is only within an Mev of the value of 167.1 Mev, since the measured value is 167.1 ± 1.6 Mev. Hence further uncertainties are introduced in the neutron emission

calculations. Therefore the overall average kinetic energy to which the time-of-flight data have been fitted represents an important source of uncertainty in the calculations.

The value assumed for the nuclear temperature also affects the calculations. Although the final calculations were done for a temperature of 0.59 Mev, it is seen in Table VI that for fission near the most probable mass ratio an increase in the nuclear temperature to 1.00 Mev causes a decrease of 0.23 neutrons in the number of neutrons per fission emitted from a fragment pair for fission near the most probable mass division. Hence the calculations are sensitive to the value used for the nuclear temperature. Although one might try a variable nuclear temperature, in view of the uncertainties in the other numbers entering into the calculations it does not seem that much could be learned by doing so.

In principle it would be possible to derive a cumulative yield curve giving the probability distribution for the mass numbers of the fission fragments after neutron emission. To do this one would use the single fragment neutron emission probabilities and the primary yield curve for the fission fragments before neutron emission derived in this work. However, in view of the uncertainties in the neutron emission probabilities and the approximate nature of the primary yield curve, this has not been done.

The results of this work illustrate the satisfactory nature of evaporation theory calculations, and, in view of the uncertainties which have just been discussed, the overall average of 2.95 neutrons per fission for the calculations using $r = 0.5$, $T = 0.59$ Mev, and $\Delta\bar{E}_T = 0$

is in good agreement with the experimental value of 2.46 neutrons per fission.

Table I. Coefficients for the Velocity Probability Surface $F_0(x,y)$.

Coefficient	Value	Maximum Absolute Value of Corresponding Term
A_0	115.792	115.8
A_{01}	-7.765	14.9
A_{20}	-0.130	2.9
A_{02}	-0.182	1.3
A_{21}	0.122	5.0
A_{12}	0.188	4.6
B	2.298	21.2

Table II. Importance of Velocity Dispersion in Heavy Fragment Velocities.

(All velocities and standard deviations are in units of 10^7 cm/sec.)

	Minimum σ_H	Most Probable σ_H	Maximum σ_H
Heavy Fragment Velocity v_H	80	96	110
Light Fragment Velocity v_L	155	141	125
Std. Dev. σ_H in Heavy Fragment Velocities	0.89	1.11	1.36
Std. Dev. Σ_H in Expt. Velocity Surface	6.53	6.53	6.53
Std. Dev. $S_H =$ $\sqrt{\Sigma_H^2 - \sigma_H^2}$	6.47	6.44	6.39
Per cent Change $\frac{\Sigma_H - S_H}{S_H}$	0.9	1.4	2.2

Table III. Importance of Velocity Dispersion in Light Fragment Velocities.

(All velocities and standard deviations are in units of 10^7 cm/sec.)

	Minimum σ_L	Most Probable σ_L	Maximum σ_L
Heavy Fragment Velocity v_H	110	96	80
Light Fragment Velocity v_L	125	141	155
Std. Dev. σ_L in Light Fragment Velocities	1.67	2.06	2.48
Std. Dev. Σ_L in Expt. Velocity Surface	5.10	5.10	5.10
Std. Dev. $S_L =$ $\sqrt{\Sigma_L^2 - \sigma_L^2}$	4.82	4.67	4.46
Per cent Change $\frac{\Sigma_L - S_L}{S_L}$	5.8	9.2	14.3

Table IV. Constants in the Total Kinetic Energy Probability Density

Functions $Q_K(E_K^t; R)$.

Heavy Fragment Mass Number A_H	Coefficient A_1	Coefficient A_2	Mean E_1 (Mev)	Mean E_2 (Mev)	Std. Dev. σ_1 (Mev)	Std. Dev. σ_2 (Mev)
127	4.71	0.96	185.1	186.1	12.70	3.39
129	11.47	2.96	181.7	181.8	11.90	3.08
131	23.65	9.15	178.9	178.9	11.00	2.92
133	38.84	23.46	175.7	176.7	11.00	2.92
135	64.91	29.74	173.1	174.3	9.75	2.34
137	88.09	20.81	170.5	171.7	9.06	2.59
139	108.12	1.65	167.7	168.2	8.45	2.67
141	107.58	1.64	165.7	166.2	8.45	2.67
143	98.31	18.22	162.9	165.1	7.81	2.47
145	79.74	35.49	160.4	162.4	7.38	2.00
147	58.20	32.92	158.4	159.3	6.96	1.82
149	38.33	18.85	155.9	155.9	6.36	1.87
151	19.26	11.35	154.0	153.5	6.78	2.00
153	11.99	2.33	151.8	150.8	5.52	1.58

Table V. Validity of Using Mean Energies in Neutron Emission

Calculations for Mass Ratio $R = 143/93$.

(All energies and the nuclear temperature are in Mev.)

The energies used in calculation 7 are the means of those used in 1-6.)

	1	2	3	4	5	6	7
Z_L	40	39	38	37	36	35	37.5
Z_H	52	53	54	55	56	57	54.5
w	0.019	0.133	0.348	0.348	0.133	0.019	1.000
B_{1L}	6.99	7.26	4.73	6.10	2.91	4.63	5.34
B_{1H}	2.56	4.62	3.37	5.14	3.98	5.86	4.27
B_{2L}	8.74	6.47	6.75	4.21	5.59	2.40	5.63
B_{2H}	4.28	3.03	4.80	3.63	5.51	4.69	4.24
B_{3L}	7.53	8.21	5.95	6.23	3.70	5.08	6.06
B_{3H}	2.68	4.45	3.28	5.16	4.34	6.15	4.27
B_{4L}	11.65	6.99	7.69	5.43	5.71	3.18	6.54
B_{4H}	4.10	2.93	4.81	3.99	5.80	5.77	4.41
B_{5L}	9.50	11.12	6.46	7.15	4.90	5.19	7.15
B_{5H}	2.58	4.52	3.63	5.44	5.42	8.38	4.69
r	0.50	0.50	0.50	0.50	0.50	0.50	0.50
T	0.59	0.59	0.59	0.59	0.59	0.59	0.59
$\bar{E}_K(Z_H, Z_L)$	166.03	164.99	163.79	162.43	160.92	159.24	163.06
E_T	176.85	183.67	187.83	187.54	184.55	177.19	186.32
n_L	0.48	0.91	1.45	1.54	1.72	1.12	1.39
n_H	1.30	1.67	2.01	1.81	1.52	0.73	1.81
n	1.78	2.58	3.46	3.35	3.24	1.85	3.20
Averages of 1-6.		Results of 7					
n_L	1.42	1.39					
n_H	1.79	1.81					
n	3.21	3.20					

Table V (cont'd)

Notes.

w is the probability weight factor

B_{iL} is the separation energy of the i th neutron in the light fragment

r is the fraction of excitation energy given to the light fragment.

Table VI. Dependence of Neutron Emission on Nuclear Temperature for Fission with Mass Ratio $R = 143/93$ (Energies in Mev.)

		1	2
Excitation Fraction	r	0.50	0.50
Nuclear Temperature	T	0.59	1.00
Mean Kinetic Energy	\bar{E}_K	163.06	163.06
Mean Total Energy	\bar{E}_T	186.32	186.32
Neutrons Emitted	n_L	1.39	1.31
	n_H	1.81	1.66
	n	3.20	2.97

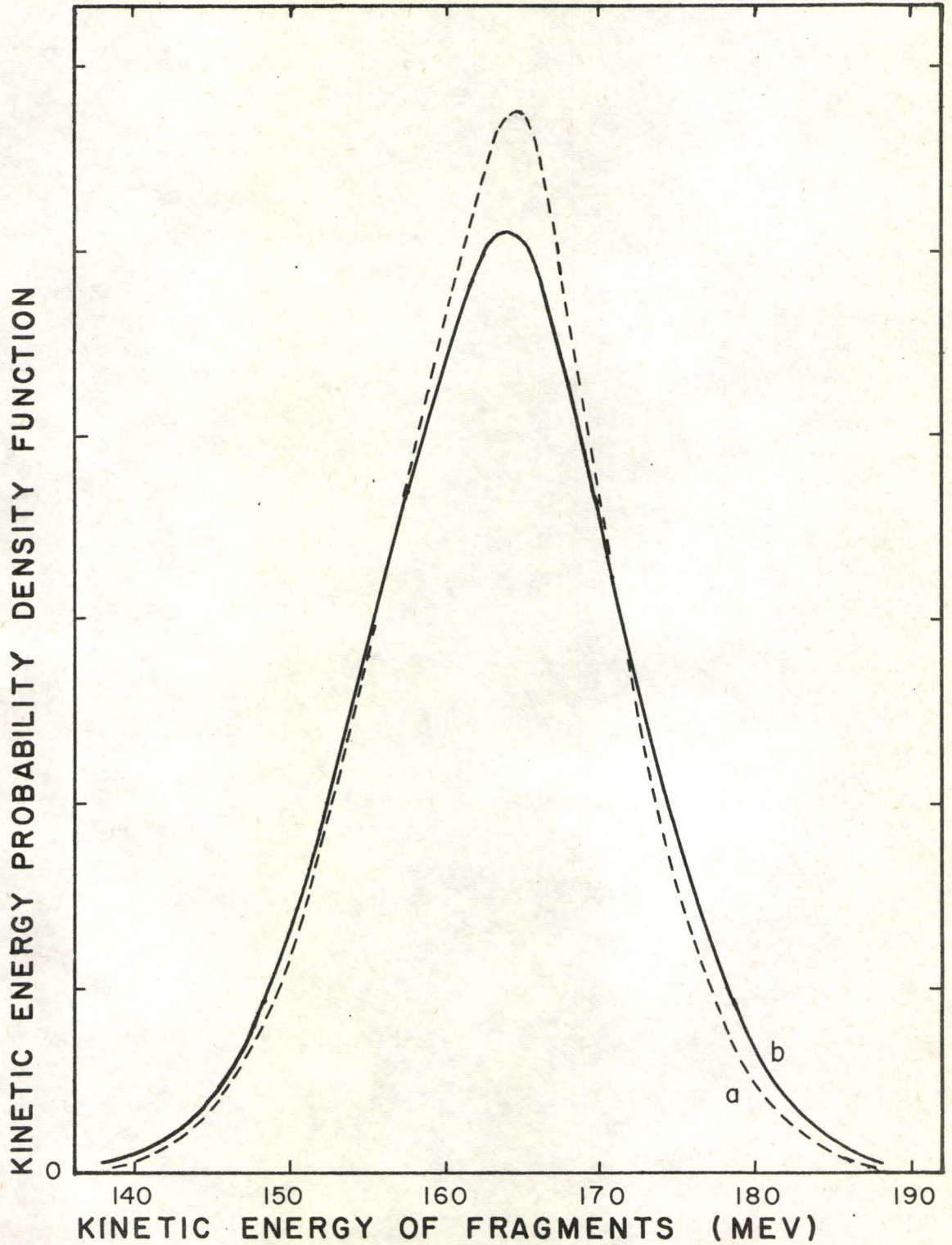
Table VII. Dependence of Neutron Emission on Excitation Energy Division for Fission with Mass Ratio $R = 143/93$ (Energies in Mev.)

		1	2	3	4
Excitation Fraction	r	0.40	0.50	0.60	0.70
Nuclear Temperature	T	0.59	0.59	0.59	0.59
Mean Kinetic Energy	\bar{E}_K	163.06	163.06	163.06	163.06
Mean Total Energy	\bar{E}_T	186.32	186.32	186.32	186.32
Neutrons Emitted	n_L	1.08	1.39	1.75	2.04
	n_H	2.29	1.81	1.40	1.00
	n	3.37	3.20	3.15	3.04

Table VIII. Dependence of Neutron Emission on Mean Total Energy Release
for Fission with Mass Ratio $R = 143/93$ (Energies in Mev.)

		1	2	3	4
Excitation Fraction	r	0.50	0.50	0.50	0.50
Nuclear Temperature	T	0.59	0.59	0.59	0.59
Mean Kinetic Energy	\bar{E}_K	163.06	163.06	163.06	163.06
Mean Total Energy Increment	$\Delta\bar{E}_T$	0	-1.50	-3.00	-4.50
Mean Total Energy	\bar{E}_T	186.32	184.82	183.32	181.82
Neutrons Emitted	n_L	1.39	1.29	1.19	1.09
	n_H	1.81	1.68	1.54	1.41
	n	3.20	2.97	2.73	2.50

FIGURE 1
DISPERSION REMOVAL FOR MASS RATIO $R = 143/93$



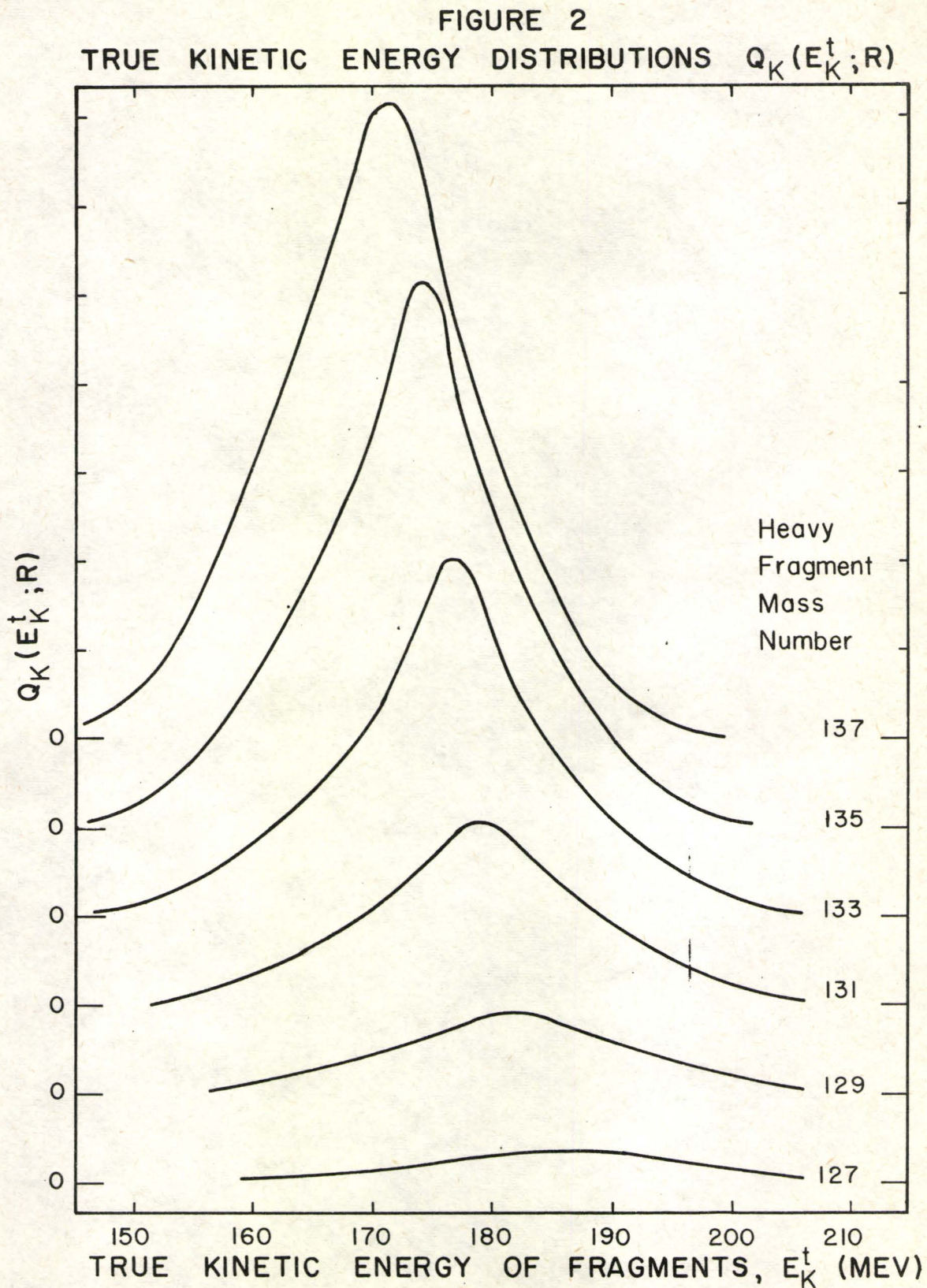


FIGURE 3
TRUE KINETIC ENERGY DISTRIBUTIONS $Q_K(E_K^t; R)$

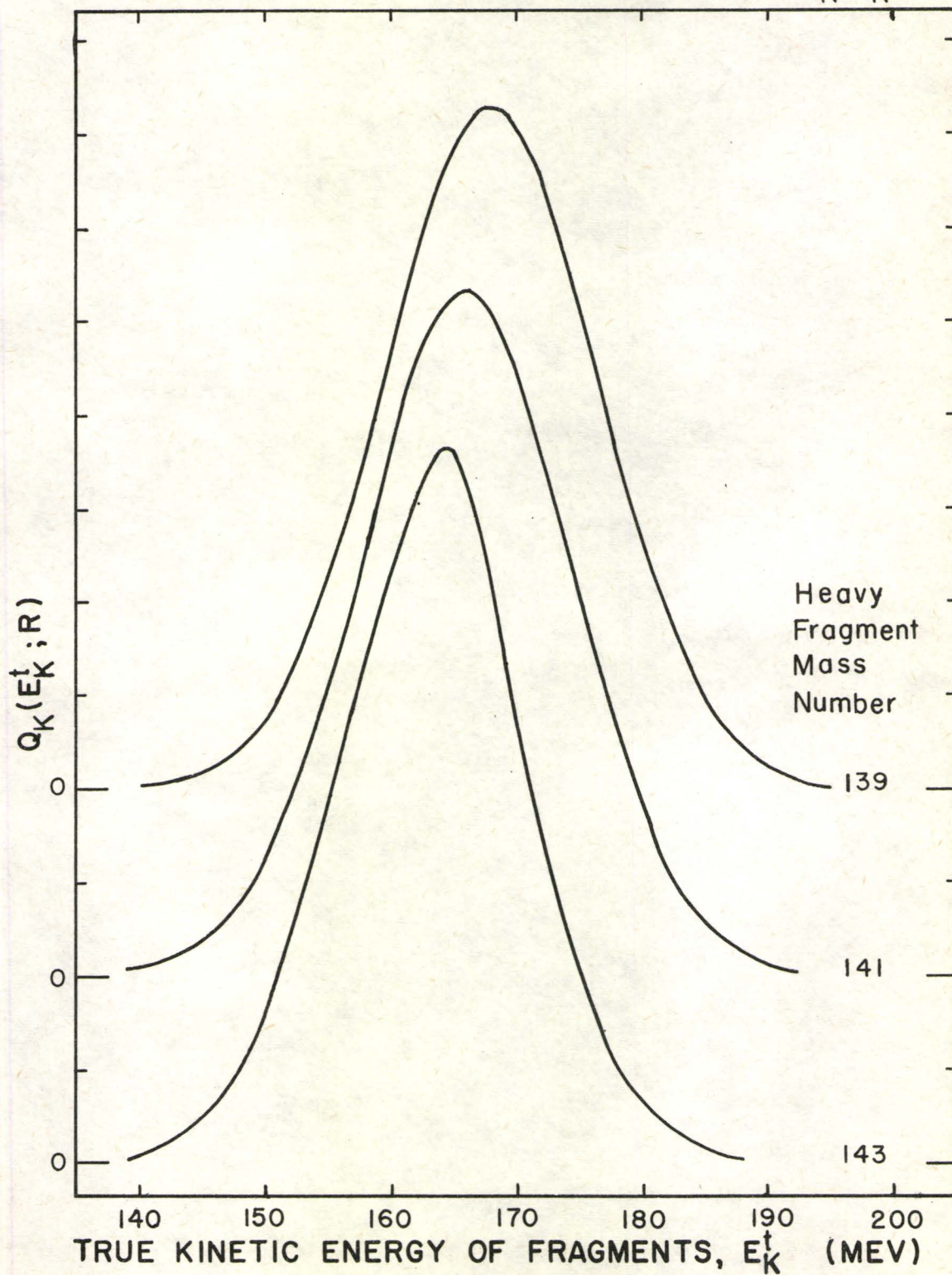
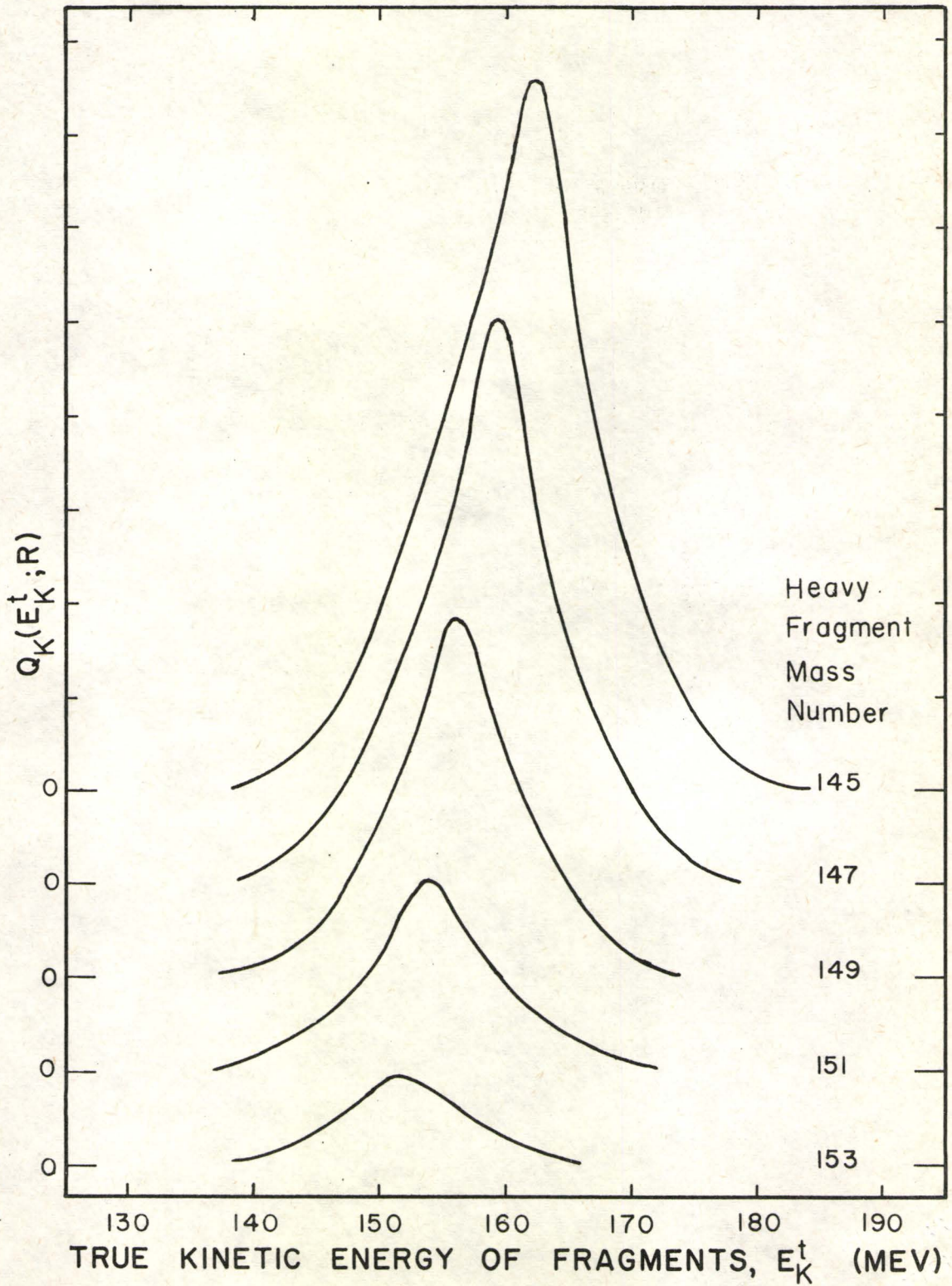


FIGURE 4
TRUE KINETIC ENERGY DISTRIBUTIONS $Q_K(E_K^t; R)$



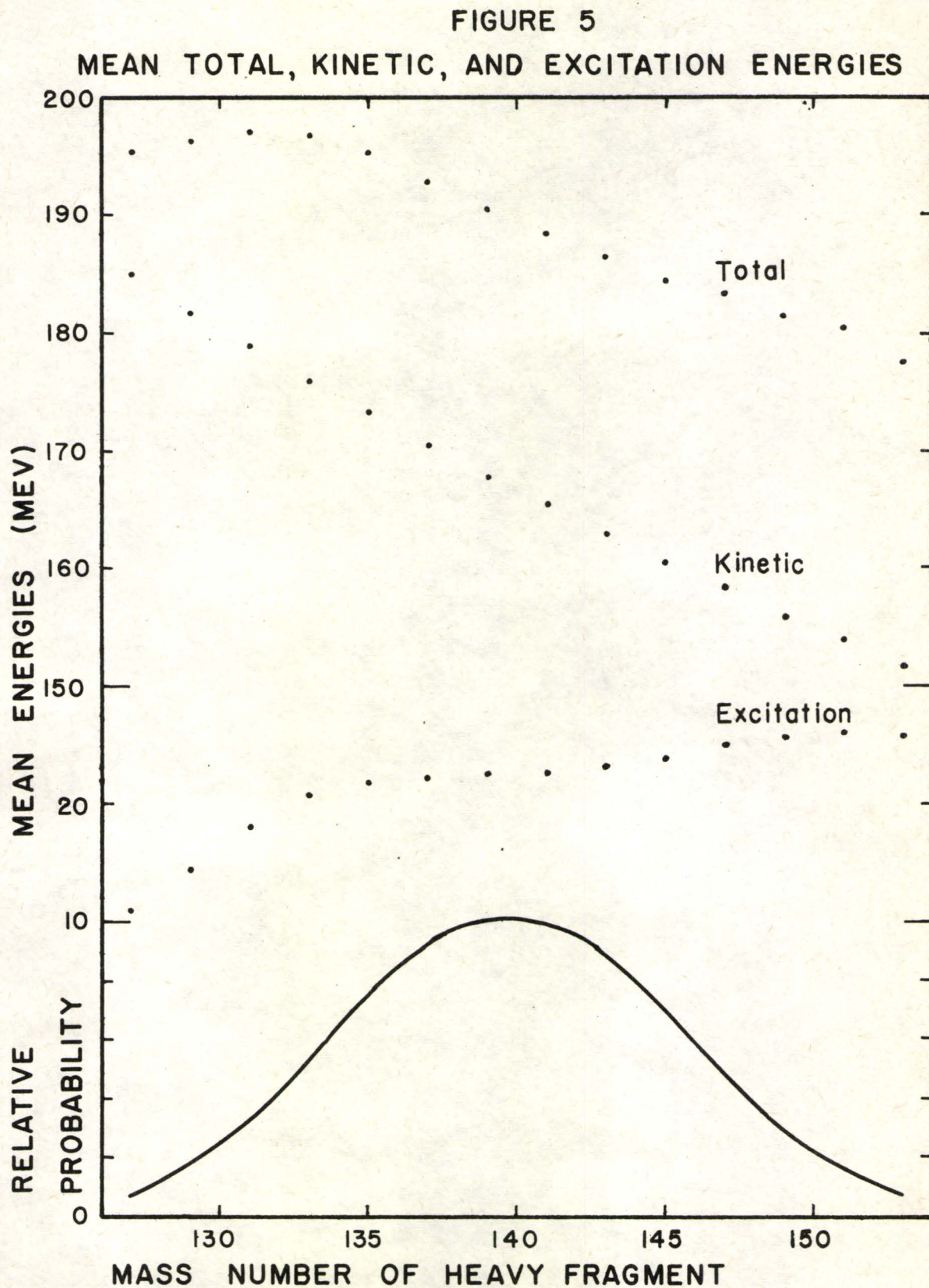
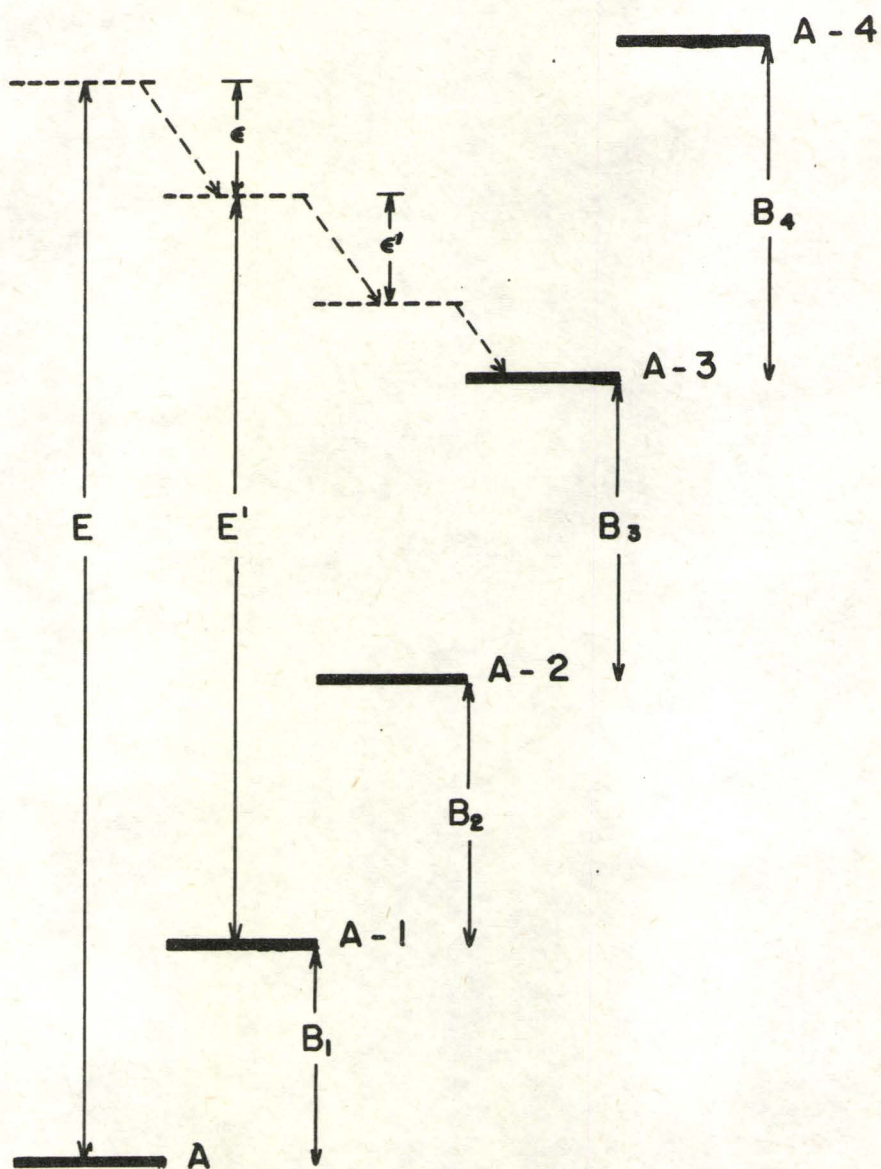


FIGURE 6
ENERGY DIAGRAM FOR $p(3; \beta_3 \neq E \neq \beta_4)$



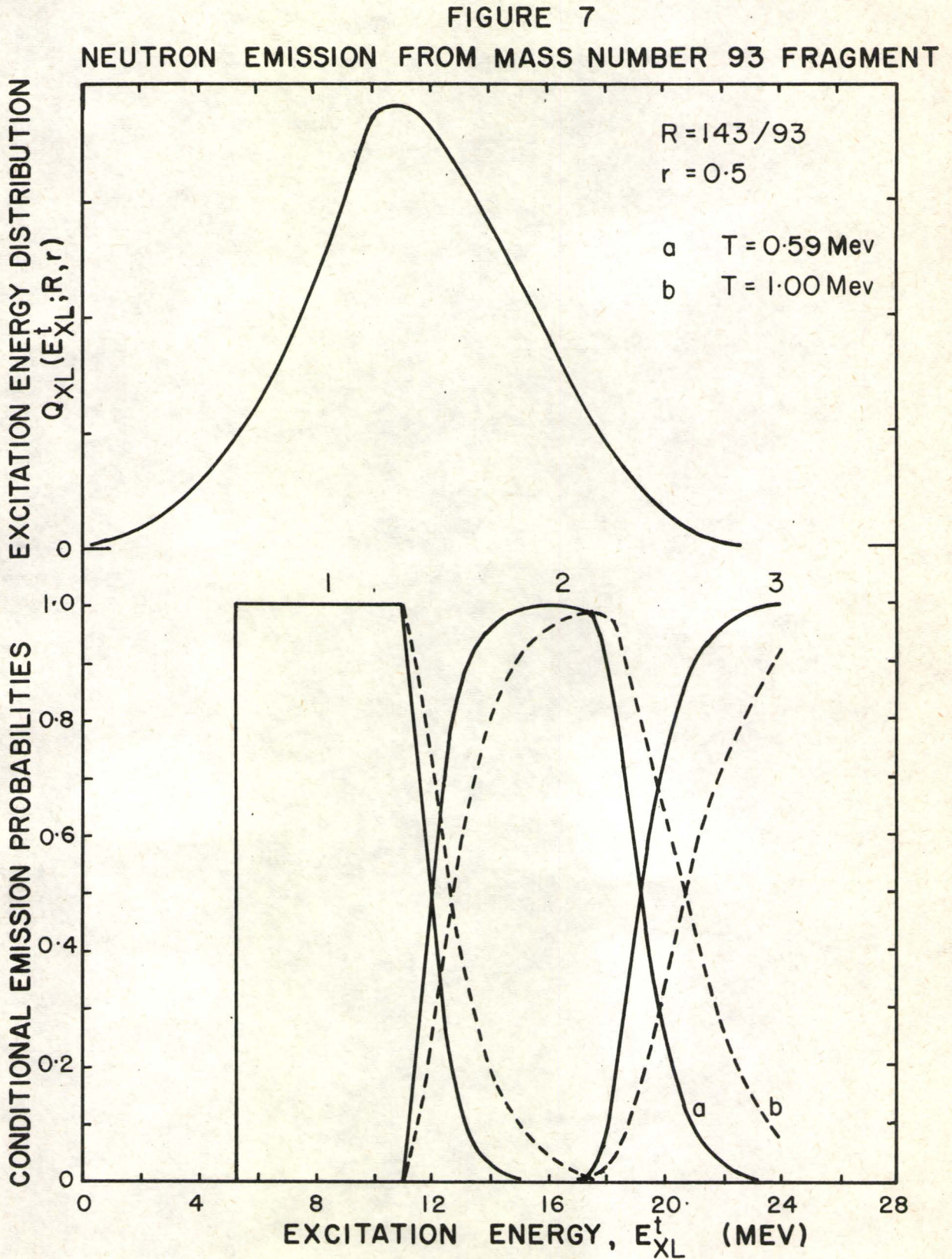


FIGURE 8
NEUTRON EMISSION FROM MASS NUMBER 143 FRAGMENT

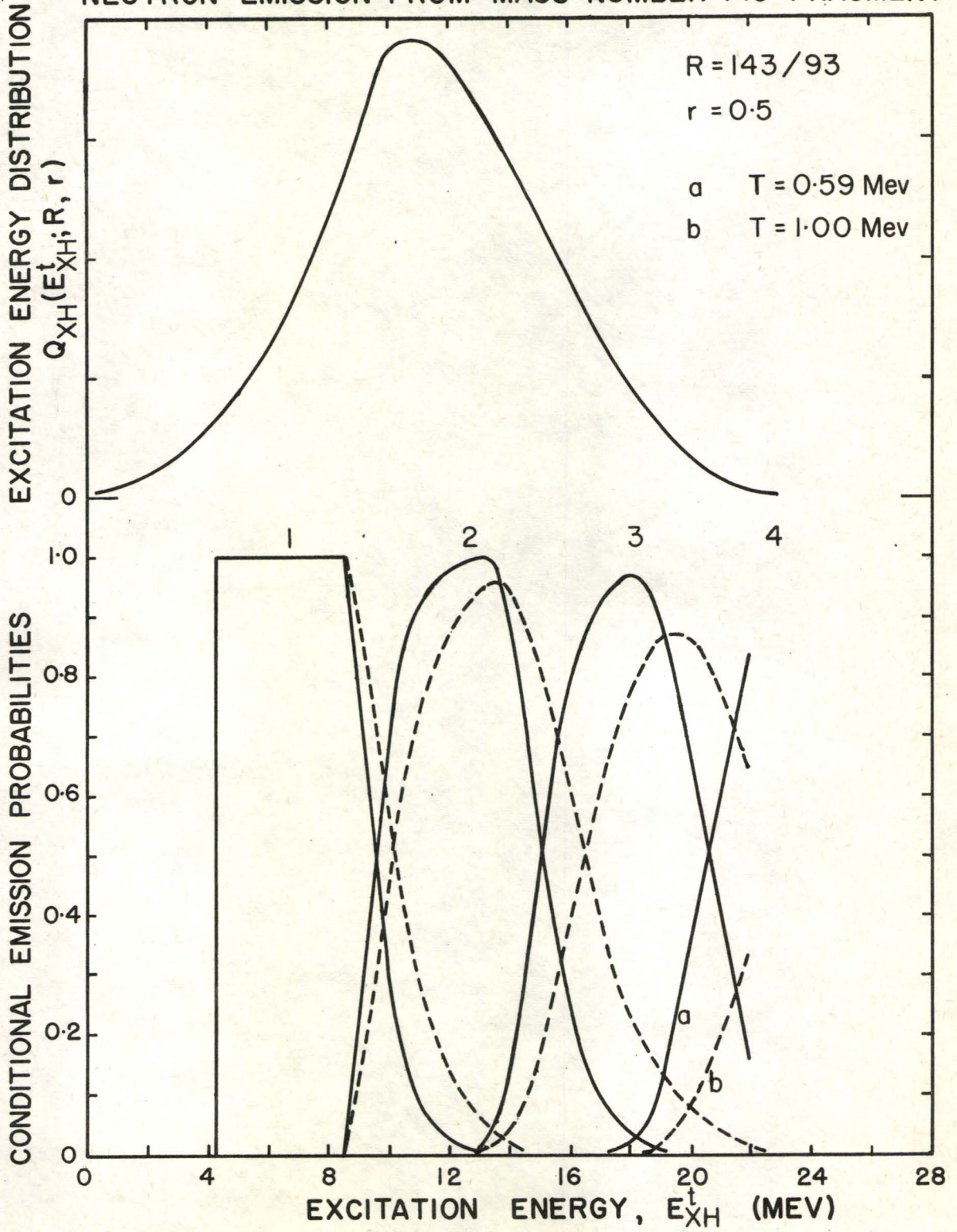
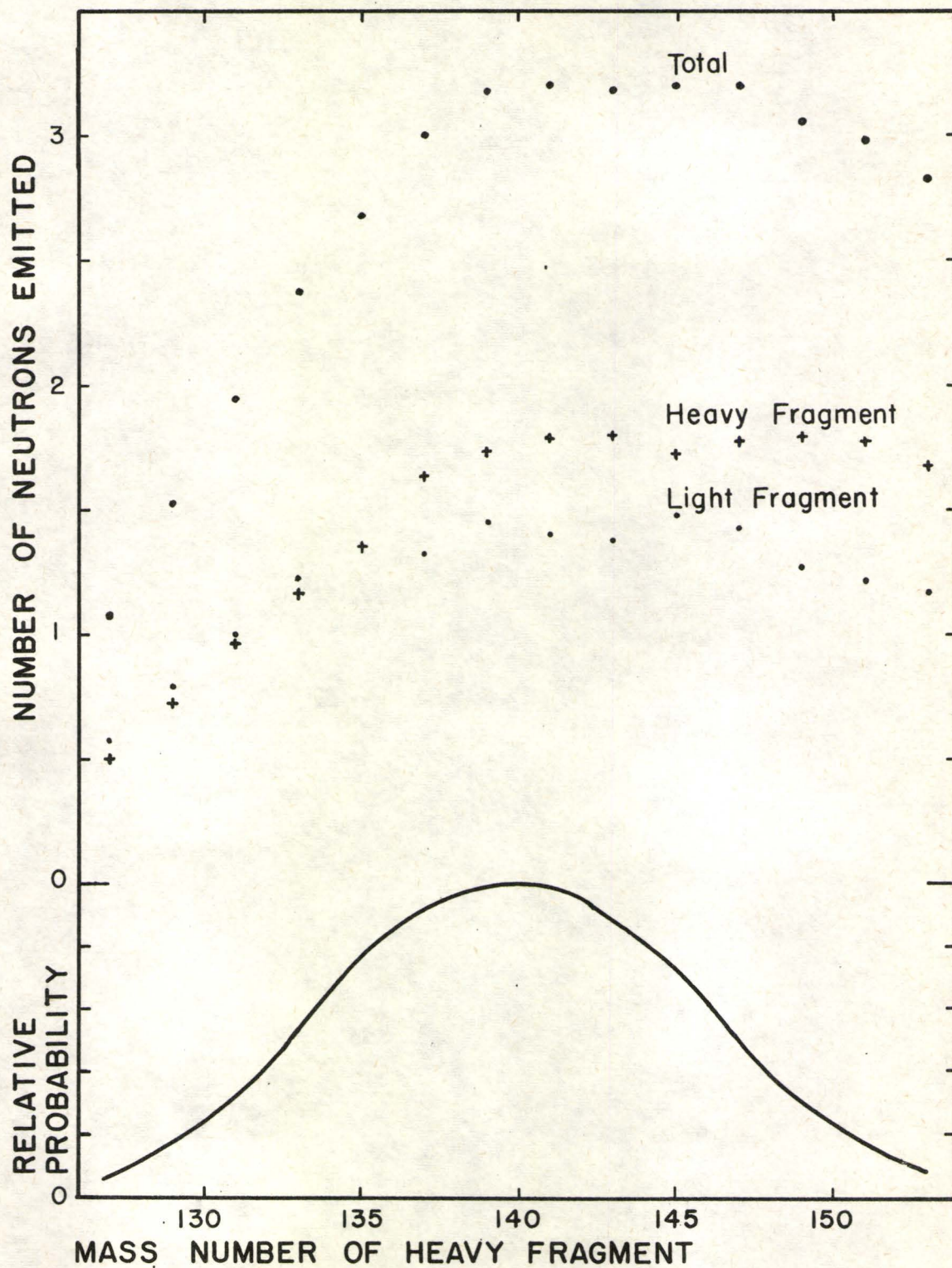


FIGURE 9
NEUTRON EMISSION USING $r=0.5$, $T=0.59$, $\Delta\bar{E}_T=0$.



Bibliography

- Blatt and Weisskopf (1952), "Theoretical Nuclear Physics" (John Wiley and Sons, London).
- Brunton, D. C. and Hanna, G. C. (1950), Can. J. Research A28, 190.
- Cameron, A. G. W. (1957), Atomic Energy of Canada Limited, Chalk River Project CRP-690 (AECL-433).
- Cohen, B. L. and Fulmer, C. B. (1958), Nuclear Phys. 6, 547.
- Demirkhanov, R. A., Gutkin, T. I., and Dorokhov, V. V. (1959), Soviet Phys. - J.E.T.P. 35(8), 639.
- Duckworth, H. E. (1957), Progr. in Nuclear Phys. 6, 138.
- Fraser, J. S. and Milton, J. C. D. (1954), Phys. Rev. 93, 818.
- Fraser, J. S. and Milton, J. C. D. (1958), Phys. Rev. 111, 877.
- Hay, I. W. and Newton, T. D. (1956), Atomic Energy of Canada Limited, Chalk River Project TPI-87.
- Huizenga, J. R. (1955), Physica XXI, 410.
- Kennett, T. J. and Thode, H. G. (1956), Phys. Rev. 103, 323.
- Leachman, R. B. (1956), Phys. Rev. 101, 1005.
- Leachman, R. B. and Kazek, C. S., Jr. (1957), Phys. Rev. 105, 1511.
- Leachman, R. B. and Schafer, W. D. (1955), Can. J. Phys. 33, 357.
- Leachman, R. B. and Schmitt, H. W. (1954), Phys. Rev. 96, 1366.
- Schmitt, H. W. and Leachman, R. B. (1956), Phys. Rev. 102, 183.
- Stein, William E. (1957), Phys. Rev. 108, 94.
- Wapstra, A. H. (1955), Physica XXI, 367, 385.
- Whetstone, Stanley L., Jr. (1959), Phys. Rev. 114, 581.
- Terrell, James (1959), Phys. Rev. 113, 527.